1 **Physico-chemical characterization of urban aerosols from specific combustion**

2 **sources in West Africa at Abidjan in Côte d'Ivoire and Cotonou in Benin in the frame**

3 **of DACCIWA program**

5 Aka Jacques Adon[1], Catherine Liousse[1], Elhadji Thierno Doumbia[2], Armelle Baeza-Squiban[3],

6 Hélène Cachier[1], Jean-Francois Léon[1], Veronique Yoboué[4], Aristique Barthel Akpo[5], Corinne

7 Galy-Lacaux[1], Cyril Zouiten[6], Hongmei Xu[1, 7], Eric Gardrat[1], Sekou. Keita[8].

9 [1] Laboratoire d'Aérologie, Université de Toulouse, CNRS, UPS, Toulouse, France

10 [2] Centre National de Recherche Météorologique/Groupe d'étude de l'Atmosphère
11 Météorologique, CNRS-Météo-France, Toulouse, France

12 [3] Université Paris Diderot, Unité de Biologie Fonctionnelle et Adaptative-RMCX, CNRS, UMR
13 8251, Paris, France

14 [4] Laboratoire de Physique de l'Atmosphère, Université Félix Houphouët-Boigny, Abidjan BPV
15 34, Côte d'Ivoire

16 [5] Laboratoire de Physique du Rayonnement, Université d'Abomey-Calavi, Abomey-Calavi,
17 Bénin

18 [6] Géosciences Environnement Toulouse, Université de Toulouse, CNRS, UPS, Toulouse,
19 France

20 [7] Department of Environmental Science and Engineering, Xi'an Jiaotong University, Xi'an,
21 China

22 [8] Université de Khorogo, Khorogo, Côte d'Ivoire.

24 Correspondence to: adonjacks@gmail.com (J. Adon) and lioc@aero.obs-mip.fr (C. Liousse)

Abstract

Air pollution in West Africa has yet to be well characterized and was one of the principal motivations of the "Air Pollution and Health" work package in the DACCIWA (Dynamics-Aerosol-Chemistry-Cloud Interactions in West Africa) program. Intensive measurement campaigns were performed in two West African capitals (Abidjan in Côte d'Ivoire and Cotonou in Benin), in order to examine the size distribution of particulate matter (PM) and their chemical composition (Elemental Carbon (EC), Organic Carbon (OC), Water-soluble organic carbon (WSOC), Water-soluble inorganic ions (WSI) and trace metals). In this study, we characterize PM from different sites in Abidjan which are representative of Domestic Fires (ADF), Traffic (AT) and Waste Burning (AWB), as well as a Traffic site (CT) in Cotonou. These sites, impacted by a large volumes of pollution, are representative of the main combustion sources in south West Africa during the dry and wet seasons. To this end, intensive campaigns were run in Abidjan and Cotonou in July (2015 and 2016) and January (2016 and 2017).

Results show a well-marked seasonality and inter-annual variabily and spatial variabilities with PM levels higher than the WHO guidelines of $25\mu g/m^{-3}$. The average mass concentrations during the wet season were 90, 104.1, 69.1 and 517.3 $\mu g.m^{-3}$ at the AT, CT, AWB and ADF sites, respectively. The largest value at the ADF site is due to the contribution of food smoking and roasting activities. In the dry season, concentrations increase to 141.3, 269.7 and 175.3 $\mu g.m^{-3}$ at the AT, CT and AWB sites respectively, whereas at the ADF site, concentrations decrease to 375.7 $\mu g.m^{-3}$.

The chemical aerosol mass closure shows that dust contributed to 25-65% of PM at both the AT, CT and AWB sites, and 10-30% at the ADF site with a clear seasonal cycle. A large variability in Particulate Organic Matter (POM) is observed, ranging from 37-68% at ADF, 20-42% at AT, 10-34% at AWB and 15-22% at CT. The contribution of WSI to bulk PM (lower than 20%) is 2-3 times larger in the wet season than the dry, except at the ADF site where no season variation is observed. The most dominant species in the WSI fraction at ADF are chloride (18-36% of the total ions), potassium (8-22%) and calcium (13-25%), while at the rest of the sites, nitrate (21-36%), chloride (6-30%) and sulfate (9-20%) are dominant. At all sites, the proportion of EC is twice as high in the dry season as in the wet season. Carbonaceous aerosol (sum of EC and POM) and dust particles are the two major contributors to the coarse,

62 fine, and ultrafine particle fractions with carbonaceous aerosol predominant in Abidjan, while
63 dust is predominant in Cotonou.

64 The highest carbonaceous aerosol contribution is observed at ADF (up to 75% of total
65 PM), while at the other sites its contribution ranges between 18 and 35%. WSOC levels are the
66 highest at the ADF site with more important values during the wet season. The concentrations
67 of WSOC at the Abidjan traffic site are higher than those recorded at the Cotonou traffic site in
68 the wet seasons, but lower in dry periods. Element trace characterization is also determined,
69 showing predominance of Al, Na and Ca followed by Fe, K and Mg.

70 Our study highlights the contribution of different traffic emissions in two major West
71 African cities to atmospheric aerosol composition. It also highlights the role of domestic fires
72 and waste combustion sources. It constitutes an original database that characterizes urban air
73 pollution from specific African combustion sources.

74 **Keywords**: DACCIWA, atmospheric pollution, size distribution, chemical composition,
75 traffic, waste burning, domestic fire, biomass burning.

76

1. Introduction

78 The impact of anthropogenic pollution on health has been demonstrated by numerous
79 studies in Europe and North America which have contributed to the implementation of emission
80 reduction policies. By contrast, air pollution in Africa is far from being well characterized,
81 although it is suspected to be responsible for negative health outcomes (WHO). This is a major
82 problem since Africa is an intense emitter of pollution including biomass burning domestic
83 fires, car traffic and growing oil and mining industries. It also has one of the fastest growing
84 populations in the world. Indeed, it has been shown that massive urbanization and rapid
85 economic growth could be responsible for tripling anthropogenic emissions in Africa between
86 2000 and 2030 (Liousse et al., 2014). This results in a major degradation of air quality and an
87 impact on the health of exposed populations. Only a few studies on this subject have been
88 conducted in Africa (Val et al., 2013; Dieme et al., 2012; Kouassi et al., 2009).

89 Because of its high atmospheric particulate concentrations already measured to be of
90 the same order as in Asian megacities and well above international standards of the WHO
91 (World Organization Health) (WHO, 2014), and due to the complex mixture of pollutants from
92 various origins, West Africa is an "unique laboratory" to study urban pollution. Previous studies

93 conducted under the framework of the AMMA (Analyses Multidisciplinaires de la Mousson

94 Africaine) and POLCA (POLlution des Capitales Africaines) programs, have revealed very

95 high pollution concentration levels in Cotonou (Benin), Bamako (Mali), Dakar (Senegal) and

96 Yaoundé (Cameroun) during the dry season, suggesting that the population may be affected by

97 negative health outcomes. For example, Val et al. (2013) showed that the inflammatory impact

98 of combustion aerosol depends on the type of emission sources and determined the predominant

99 role of particulate organic matter. Moreover, fine and ultrafine aerosol fractions, as well as

100 specific compositions including trace metals and organic compounds, have been shown to

101 induce biological effects due to their ability to reach the distal lung (Cassee et al., 2013). Such

102 reasons highlight the need to better understand the size-speciation of aerosol chemical

103 composition for the main African anthropogenic sources during the different seasons. In this

104 context, the DACCIWA (Dynamics-Aerosol-Chemistry-Cloud Interactions in West Africa)

105 program, dedicated a specific work package to "Air Pollution and Health" dealing with

106 pollutant characterization related to health issues through toxicological studies and

107 inflammatory risk modeling. The strategy was to measure aerosol chemical composition in two

108 typical traffic-sampling sites, one in Abidjan (Côte d'Ivoire) and another one in Cotonou

109 (Benin), which differ in terms of fleets, type of fuel used and quality of roads.

110 In Cotonou, the majority of the population uses motorbikes for transportation, whereas in

111 Abidjan the vehicle fleet is dominated by diesel engines. Measurements were also performed

112 at domestic fire and waste burning sites, both located in Abidjan. Intensive campaigns have

113 been organized during both the dry and wet seasons of January 2016 and 2017 in Abidjan and

114 Cotonou. In this paper, we present the aerosol chemical results for these cities and the different

115 studied combustion sources: (i) PM size distribution and mass concentrations and (ii) PM

116 chemical composition including carbonaceous aerosol, water-soluble organic carbon, water-

117 soluble inorganic ions, dust and trace elements for coarse, fine, ultrafine particles will be

118 detailed for all sites.

119

2. Experimental method

2.1. Experimental sites

122 Four measurement campaigns have been performed in July 2015 (07/20-26 period-wet

123 season) and January 2016 (01/7-15 period-dry season), July 2016 (07/4-13 period-wet season),

124 and January 2017 (01/5-14 period-dry season) at Abidjan (Côte d'Ivoire) and Cotonou (Benin)

125 at the four different source sites: ADF for Abidjan Domestic Fires, AWB for Abidjan Waste

126 Burning, AT for Abidjan Traffic (Figure 1) and CT for Cotonou Traffic site (Figure 2).

127 The ADF site is situated in Yopougon Bracody district near a market (5˚ 19 '44 "North, 4˚ 06'

128 21" West) (Figure 1). This geographical area is highly populated with various small commercial

129 activities such as a fish and meat-smoking by women which gives rise to air pollution. There

130 are also many formal and informal settlements, which mainly use wood and charcoal as a source

131 of fuel for private and professional activities. Other sources of concern contributing to the mix

132 of pollutant emissions in the area include transportation-related emissions, biomass burning,

133 garbage bins or small landfills, and various other fugitive sources.

134 The Abidjan traffic site, (AT) is located in Adjamé, on the roof of « 220 pharmacie logement

135 building » (5° 21' 14" N, 4° 01' 04" W), 10 m above ground level, and roughly 10 m away from

136 the main road. This site, close to the Adjamé market and to a bus station, is thus highly affected

137 by traffic (Gbaka, bus, taxi, woro-woro, personal cars…). The Abidjan waste Burning site

138 (AWB) (5° 21' 12" N, 3° 56' 16" W) is located at Akouédo in the district of Cocody, on the roof

139 of « Talafiguié », a building 15 m above ground level. This site is close to the big waste burning

140 area of Abidjan established in 1965, which covers an area of 153 ha.

141 The Cotonou Traffic (CT) (6° 22' 19" N, 2° 26' 5.143" E) site is located in Cotonou, on the

142 «Sogema» building roof, 4m above ground level. This site is close to the Dantokpa market and

143 also to the biggest crossroad of Cotonou (intersection of 4 main roads). This site is highly

144 influenced by traffic activities. It is important to note that vehicle fleet and fuels are different

145 in Cotonou than in Abidjan since (1) there are many two-wheel vehicles in Cotonou, (2) in

146 Cotonou, gasoline is of poor quality due to the illegal fuel transport from Nigeria (Figure 3) and

147 (3) the roads are in worse condition in Cotonou than in Abidjan.

148 **2.2. Measurements**

149 The collection of aerosol filter samples was performed with three cascade impactors,

150 operating in parallel for 3 hours over three days for each intensive campaign to allow size-

151 speciated characterization of the aerosol chemical composition. The first 4-stage impactor

152 included 4 quartz fiber filters (QMA, Whatman), for carbonaceous aerosol (EC, OC and WSOC

153 analysis), with three filters of 47mm size for the upper stages and 1 of 70 mm for the lower

154 stage. The second 3-stage cascade impactor was equipped with three Teflon filters (Zefluor,

155 Pall Corporation®) of 25 mm size and was dedicated for aerosol mass, water-soluble ions

156 species and trace elements. Finally, the third 4-stage cascade impactor dedicated to
157 toxicological analyses and whose results are not used in this paper, was mounted with four 47
158 mm diameter filters and a 70 mm filter in Nuclepore polycarbonate filters quality (porosity 1
159 µm).

160 Note that filters were punched in each case to allow a UF (< 0.2 µm), F [(0.5-0.2 µm) and C (>2.5-
161 1 µm) classification. Chemical characterization included aerosol mass, EC, OC, Water Soluble
162 Organic Carbon, Water Soluble Ionic species and trace elements.

2.3. Analyses

2.3.1. Gravimetric analyses

165 Aerosol mass concentrations are obtained using a high-precision balance (SARTORIUS
166 MC21S) in Toulouse, France, at Laboratoire d'Aérologie, placed under a controlled
167 temperature and humidity atmosphere (Person and Tymen, 2005). Before weighing, the filters
168 are kept about for 24 hours in the weighing room at an ambient relative humidity of 30 ±15%.
169 The filters are weighed before and after sampling. Result of a gravimetric measurement consists
170 of the average of 2 to 4 weighings whose differences do not exceed 5µg. The standard error on
171 a gravimetric measurement is therefore less than 10 µg, typically representing less than 5% of
172 the particles mass.

2.3.2. Carbonaceous aerosols

174 Carbonaceous aerosol is obtained from a thermal analysis with a two-step method
175 adapted from Cachier et al. (1989). Two aliquots of the same filter are separately analyzed.

176 One portion is directly analyzed for its total carbon content (TC). The other portion is
177 first submitted to a pre-combustion step (2 h at 340°C under pure oxygen) in order to eliminate
178 OC, and then analyzed for its BC content. Organic carbon (OC) concentrations are calculated
179 as the differences between TC and BC. Note that the aerosol carbon content is quantified by a
180 non-dispersive infrared (NDIR) detector with G4 ICARUS instrument with a detection limit of
181 the order of 2 µgC/cm². Uncertainty is of the order of 5% for TC, whereas in the range of 5-
182 20%, for BC and OC, depending on the sites.

2.3.3 Water Soluble Organic Carbon analysis

184 WSOC measurements are performed using a total organic carbon analyzer (Sievers M9).
185 A detailed description of this technique is reported in Favez et al. (2008). Briefly, in this

186 instrument, the full oxidation of organic carbon into CO_2 is obtained by coupling chemical

187 oxidation (with ammonium persulphate) and UV light. CO_2 is then quantified by conductivity.

188 Analyses are conducted on 20 ml of solution extracts. For ultrafine samples, solutions to be

189 analyzed are obtained using a total filter surface of 3cm² (6x0.5 cm² punches symmetrically

190 taken out of each QMA filter), whereas, for coarse and fine sizes, due to the geometry of the

191 spots formed at the surface of the filters, samples are divided into equivalent parts (1/2 or 1/4

192 of filters, rest of carbonaceous analysis). The extraction protocol consists in 16h soaking under

193 soft shaking in an Erlen-Meyer containing 20mL of ultra-pure water. Prior to WSOC analysis,

194 water extracts are filtered through Teflon (PTFE) filters (0.2μm pore size diameter) in order to

195 remove any suspended particle. Measurement uncertainty, given by the manufacturer, is of the

196 order of 7%. The overall calculated blank value is of the order of 2.27 ± 0.33 µgC/cm², which

197 represents $16.4 \pm 8.5\%$ of the mean WSOC content. For each sample, duplicate analyses showed

198 a good reproducibility.

2.3.4 Water-soluble ionic species

200 Water-soluble ionic species (Na^+, NH_4^+, K^+, Mg^{2+}, Ca^{++}, SO_4^{2-}, NO_3^-, Cl^-) are analyzed using

201 ion chromatography (IC) analyzer, following the analytical protocol described in Adon et al.

202 (2010). Briefly, the aerosol water-soluble fraction is first extracted from half Teflon filter (the

203 other part is used for trace element analysis), with a 10 min sonication in plastic vials including

204 6 ml or 10 ml of purified water (with a controlled resistivity of 18.2MΩ). Then such vials are

205 submitted to ionic chromatography analysis or stored at +4°C if not analyzed immediately.

206 Cations are analyzed with Dionex DX-100 and anions with Dionex DX-500 with a detection

207 limit of 1 to 6 ppb depending on ionic species. Uncertainties in the range of 1-50% is found

208 depending on ionic species.

2.3.5 Trace elements

210 Half sampled Teflon filters are mineralized by acid digestion with a 10 ml concentrated

211 HNO_3 and 0.5 ml HF solution (Lamaison, 2006) using a closed vessel microwave accelerated

212 reaction system (MARS 5, CEM Corporation) at high pressure (700 psi) (Celo et al. 2010). The

213 digestion is realized in 3 steps: a rise in temperature at 130°C in 3min and holding for 1 min,

214 then, a second rise at 160°C in 1 min and holding for 30 seconds and finally a third rise to

215 180°C in 1 min and holding for 3min. After a 12 h cooling period, the solutions are evaporated

216 at 80°C, and concentrated in 7 ml of 2% concentrated HNO_3 solution, before analysis by ICP-

217 MS. This protocol is developed and performed at the Laboratory of Environmental Geosciences

218   of Toulouse. ICP-MS analyses are performed with a 7500 ce Agilent Technologies instrument

219   equipped with a collision cell, and using In and Re as internal standards. Quality control and

220   measurement performance are checked using NIST SRM 1648 ''Urban Particulate Matter''.

221   The detection limit is less than 10 ppt. For all the samples, the final blank values and detection

222   limit on filters are taken into account for final concentrations calculations. 13 trace metals are

223   considered in this work: Al, Ti, Cr, Mn, Fe, Ni, Cu, Zn, Ba, La, Th, Pb, and Cd.

2.3.6 Dust calculation

225   Many methods can be used to quantify the dust concentrations in our samples.

226   (1)   Sciare et al. (2005) methodology consists in using soluble calcium data obtained with

227   Ionic Chromatography (IC) to estimate Dust mass following the relationship:

228   Dust = 10.96 ± 1.00 [nss-Ca^{2+}], where nss-Ca^{2+} (=$1.02*Ca^{2+}$-$0.038*Na^{+}$) refers to non-sea-salt

229   calcium concentration.

230   (2)   Pettijohn (1975) and Besombes et al. (2001) propose the following equation:

231   Dust = 2.20[Al] + 2.49[Si] + 1.63[Ca] +1.42[Fe] + 1.94[Ti]

232   (3)   Terzi et al. (2010) used this one:

233   Dust = 1.89[Al] + 1.21[K] + 1.95[Ca] +1.66[Mg] + 1.7 [Ti] +2.14[Si] + 1.42[Fe].

234   In our study, all these elements needed for (2) and (3) have been determined except Silica (Si).

235   Consequently, we used different relationships available in the literature to determine mean Si

236   values ($SiO_2 = 3*Al_2O_3$ mass ratios (Alastuey et al., 2005), Si = $4.0*Al$ (Zhang et al., 2003) and

237   Si = $2.03*Al$ (Chiapello et al., 1997)).

238   (4)   Guieu et al (2002) relationships are based on Al or Fe:

239   [Al] (%)=7.09 ± 0.79[dust]

240   [Fe] (%)=4.45 ± 0.49[dust]

241   (5)   Guinot et al. (2007) approach is based on a chemical closure method based on

242   reconstructed aerosol mass from EC, OC, WSI, Ca^{2+} concentrations and weighed aerosol mass.

243   Briefly, Ca^{2+}-to-dust conversion factor (f) is obtained by arbitrary fixing OC-to-POM

244   conversion factor (k) to 1.8 and by performing a linear regression between Ca^{2+} concentration

245   and the missing mass (difference between the reconstructed and weighed mass). The slope of

246   this regression represents the factor f. Based on this methodology, f ranges from 0.015 to 0.15

247   in the wet season and from 0.006 to 0.07 in the dry season in our sites. Note that at all of our

248   sites, the correlation between Ca^{2+} and missing mass is sufficiently good (r^2=0.9) to support the

249   consistency of this simple approach for the evaluation of dust. These f values are included in

250 the range of values provided in the literature (He et al. 2001; Sun et al. 2004; Guinot et al.

251 2007).

252 The results of dust masses estimated from the six methodologies described above are

253 summarized in the Table 1 for WS2016 and DS2017. Indeed, Ca, Al, and Fe concentrations

254 measured by ICP-MS are only obtained in WS 2016 and DS 2017 due to experimental

255 problems, whereas Ca^{2+} concentrations measured by IC are available for all campaigns. As a

256 result, the dust obtained from Ca^{2+} measured by IC (Sciare et al., 2005 and Guinot et al., 2007)

257 is lower than that obtained from Al and Fe by Guieu et al. (2002), by Pettijohn (1975) and by

258 Terzi et al. (2010). In addition, dust obtained from Al is generally higher than that of Fe.

259 Such comparison seems to be in agreement with methodological aspects. Indeed, Al, Fe, Ca

260 obtained by ICP-MS include both soluble and insoluble particles whereas Ca^{2+} measured by IC

261 only include soluble particles. Comparison of Ca^{2+} measured by ICP-MS (not shown here) is

262 effectively higher than that of the CI, by a factor of 1.7, 1.8, 2.2 and 1.1 in dry season, at the

263 ADF, AWB, AT, and CT sites respectively. By contrast, this factor is constant (1.3) in the wet

264 season for all the sites.

265 In our study, due to the lack of trace element data for the WS2015 and the DS2016, dust

266 estimations will be performed from Sciare et al. (2005) methodology. This is the most direct

267 one, taking into account available chemical data. The one of Guinot et al. (2007) will be used

268 for aerosol chemical closure.

2.3.7 Aerosol chemical closure methodology

270 As mentioned previously, aerosol chemical closure is performed following the Guinot

271 et al. (2007) methodology. Aerosol is separated into four components: EC, POM, water-soluble

272 ionic species and Dust. EC is directly given by thermal analysis as shown earlier. WSI is the

273 sum of all ionic species obtained by ionic chromatography. Particulate organic matter (POM)

274 values are obtained from our OC concentrations with a POM/OC ratio in the range of 1.2 to 2.1

275 whereas dust is derived from Ca^{2+} and linear regression between reconstructed and weighed

276 aerosol masses.

277

2.4 Meteorological conditions

279 Figure 4 shows meteorological data, provided by the NOAA Integrated Surface database

280 (ISD; see https:// www.ncdc.noaa.gov/isd, last access) and the ASECNA (Agence pour la

281 Sécurité de la Navigation Aérienne en Afrique et à Madagascar).

282 Our study area is under the influence of the Convergence Zone of two air masses of a different

283 nature: harmattan (hot and dry continental trade winds) from the north and monsoon (humid

284 maritime trade winds) from the south (Figure 4). Ground contact between these two air masses

285 constitutes the intertropical front (FIT) whose fluctuations during the year determine the

286 seasons in the Gulf of Guinea (Tapsoba, 1997). During the winter (dry season), temperatures

287 are relatively high with maximum around 30°C on the coast. The humidity is low, since the

288 prevailing Harmattan wind blows from the desert, usually bringing dust (Figure 4). The period

289 from June to September, especially in July is the wet season period when daytime temperatures

290 are slightly lower, with maximum around 26/28°C on the coast. The humidity level is high

291 everywhere. Rains may be abundant from April to October but also in March, November, and

292 December on the coast.

293 As depicted in Figure 4 which shows the meteorological conditions during our four campaigns,

294 temperatures are roughly the same at Abidjan and Cotonou, reaching 28°C and 26°C in the dry

295 and wet seasons, respectively. The wind direction is relatively stable in summer and winter,

296 except in January 2016 when there were slight variations. In addition (not shown here), our dry

297 season periods are particularly dry with January rainfall lower than 3 mm. Also, precipitation

298 during the wet season of 2015 was roughly similar to that of the wet season of 2016 in Abidjan

299 and Cotonou.

2.5 Backward trajectories

301 Air mass trajectory study is a very important tool to reconstruct the path of an air mass

302 for the days preceding its arrival at the sampling site. The air mass trajectories used in this study

303 are calculated with a model (READY Transport & Dispersion Modeling) developed at the Air

304 resources laboratory. The Hybrid Single-Particle Lagrangian Integrated Trajectory (HYSPLIT)

305 modelling system (Draxler and Rolph, 2012) is used for the trajectory analysis. Global Data

306 Assimilation System reanalysis database is used as meteorological input, with a 0.25×0.25

307 degrees horizontal resolution. In our study, the HYSPLIT model is run to compute 120 h back

308 trajectories ending at Abidjan and Cotonou at 1000 m a.g.l. (Figure 5).

309 As expected in January, the air masses mainly came from the north (Figure 5) and some from

310 the south-west, whereas in July the air masses came from the south-west and the south.

311 Therefore, in January, Abidjan and Cotonou are mainly impacted by polluted air masses from

312 surrounding areas and northern countries with possible dust and biomass burning influences,

313 whereas in July, the impact of cleaner air masses coming from the sea may be observed.

314

3. Results and discussion

3.1. Aerosol size distribution and mass concentration

Figure 6 shows the relative mass distribution of PM for Coarse (C), Fine (F) and Ultra-Fine (UF) particle sizes, with their average by site, for each season and campaign in Abidjan and Cotonou. Bulk concentrations, shown in Figure 6, vary widely from site to site and from year to year. During the wet season, the average total concentrations range from 82.1 to 676.3 $\mu g.m^{-3}$ in 2015 and 56.3 to 358 $\mu g.m^{-3}$ in 2016, with the maximum at the Abidjan Domestic Fire (ADF) site. While during the dry season, values range from 168.2 to 269.4 $\mu g.m^{-3}$ in 2016 and from 114.4 to 558.8 $\mu g.m^{-3}$ in 2017, with maximum concentration obtained at the Cotonou Traffic (CT) and ADF sites. In terms of size distribution, concentration peaks may be observed for the three aerosol size-fractions, ultra-fine (UF), fine (F) and coarse (C), which are found to exhibit different seasonal patterns. UF particles (< 0.2 µm) represent the highest contributor to the bulk mass at the ADF site, by up to 60 % (335.3 $\mu g.m^{-3}$) in the dry season 2017. F particles (1-0.2 µm) are the second most important contributor and both combined particle sizes account for more than 70 % of the total mass at the ADF site. Ultra fine and fine fraction are also found to be maximum during the wet season in 2015 and 2016 by up to 47 and 44%, respectively. These results highlight the importance of pollution at the ADF site in Abidjan, which is dominated by particle sizes less than 1 µm that are known to be particularly harmful to health (Kim et al., 2003; Wilson et al., 2002). Val et al. (2013) also indicates that combustion sources such as domestic fire contributes to the high toxicity of F and UF particulate matters of African urban aerosol. When looking at the seasonal variation for a full year i.e. 2016, the bulk mass is twice as high in wet season than in the dry season at the ADF site. This could be related to activities such as women drying fish and meat before selling them who use wood combustion; in wet season the woods are moist and combustion is highly incomplete, producing a large amount of smoke.

Bulk aerosol concentrations measured at the Abidjan Waste Burning (AWB) site in summer and winter 2016 are 56.3 and 173.8 $\mu g.m^{-3}$, respectively, which suggests less waste burning activities during the wet season. Also, the total concentrations obtained during the wet season of 2015 and 2016 were always lower than during the dry season of 2016 and 2017. It is also observed that at the AWB site, PM mass concentrations are mainly distributed in C mode (30-44%) over the entire period of study excepted during the wet season of 2015, and to a lesser extend in F mode (21-44%).

347   Note that the concentrations obtained at the AWB site (82.18 µg.m⁻³) are the lowest compared

348   to all sites. This could be explained by the proximity of the site to the studied source (here waste

349   burning source) which is more important than in the other sites.

350   Now, if we focus on traffic sites (Figure 6), the Cotonou traffic site aerosol concentrations are

351   higher by a factor of 1.5 to 2 than those of Abidjan traffic, especially in the dry season. Note

352   that this poor air quality found in Cotonou has recently been reported by Cachon et al. (2014).

353   The higher values found in Cotonou could be due to the more intense traffic in Cotonou than in

354   Abidjan which is associated with the lack of public transportation and the use of highly polluted

355   mopeds (aged over 15 years) (Gounougbe, 1999; Avogbe et al., 2011), despite the effort in the

356   last 10 years to restrict their use. Several studies such as MMEH (2002) have shown that more

357   than 94,000 mopeds and 350,000 second-hand vehicles are in circulation in Cotonou. Other

358   factors contributing to the local pollution include outdoor restaurants using charcoal and

359   motorcycle garages which are more present around the Cotonou site than at the Abidjan site.

360   However, the differences in concentrations between the two traffic sites are less important

361   during the wet season than during the dry season when concentrations are always higher.

362   Therefore, another factor, typical of the dry season should explain the differences between

363   concentrations. One such factor is the influence of long-term imported sources. Indeed, the

364   occurrence of continental air masses is more important in the dry season than in the wet season.

365   Some expected PM components such as dust or biomass burning particles would then appear

366   to be relatively more important in Cotonou than in Abidjan. This will be discussed in more

367   detail later.

368   In terms of PM 2.5, the conclusions are the same. The average mass concentration of PM2.5

369   over the dry season (2016-2017) are 154.30 ± 73.99, 143.8 ± 41.6, 134.1 ± 6.7 and 211.1 ± 50.9

370   µg.m⁻³ and 337.5 ± 23.8, 44.8 ± 2.9, 52.3 ± 3.8 and 70.0 ± 0.8 µg.m⁻³ over the wet season (2015-

371   2016) at the ADF, AWB, AT and CT sites, respectively. The increase in PM2.5 is of the order

372   of 54% at ADF from dry to wet season, whereas a sharp reduction (more than 60%) is obtained

373   at AWB, AT, and CT sites. As shown previously, such differences in PM2.5 concentrations

374   between the sites can be explained by (1) the source specificity with more or less incomplete

375   combustion: wood combustion and two wheel vehicle emission factors are higher than gasoline

376   emission factors (Keita et al., 2018), (2) the proximity between the sites and the sources: the

377   ADF sampling site is much closer to the studied sources than the traffic or waste burning

378   sampling sites (3) the relative influence of transported sources to the studied sites such as dust

379   and biomass burning (4) the occurrence of continental air masses, (5) the decrease of the

380   boundary layer height (as reported by Colette et al., 2007), (6) wet deposition of particles and

381   (7) the meteorological conditions (temperature and relative humidity).

382   It is interesting to underline that all of these values are well above the annual and daily WHO

383   guidelines of 25 and 10 µg/m³ respectively, whatever the season and the size; this is a warning

384   signal for pollution levels in African capitals if nothing is done to reduce emissions in the future.

385   Finally, it is interesting to compare our results with other DACCIWA results, including other

386   time sampling. Firstly, Figure 7 presents comparisons between our PM2.5 mass concentrations

387   and those obtained by Xu et al. (2019) from personal samplers collected in the same area and

388   at the same dates in 2016 during 12 h from women at the ADF site, students at the AWB site

389   and drivers at the CT site. We note that PM2.5 directly measured on women are 2.3 and 0.9

390   times higher than our values obtained at the ADF site in dry and wet seasons, respectively, and

391   3.40 and 4.9 times higher on students than at the AWB site, and 1.6 and 2.1 times higher on

392   drivers than at the CT site.

393   Secondly, Figure 7 presents a comparison between our values and Djossou et al. (2018) weekly

394   measurements at the same sites. It is interesting to note that our values are on average 1.6, 3, 5

395   and 8 times higher than those of Djossou et al. (2018) at the AWB, ADF, AT and CT sites

396   respectively. As it may be seen, the lowest concentrations are observed in Djossou et al. (2018),

397   whereas the highest concentrations are recorded in Xu. et al. (2019). This is valid for all sites,

398   seasons and campaigns. Differences between our values and Djossou values may be explained

399   by the sampling times of the two studies. Indeed, Djossou measurements are weekly, taking

400   into account diurnal activities during all the week, including week-end and nights which have

401   expected lower PM2.5 concentrations. Our study includes only maximum pollution conditions

402   for each site. The highest differences occur for the traffic sites. This may be clearly understood

403   since diurnal and weekly variations of traffic sources are the most variable. Comparison

404   between our values and Xu et al. (2019) values is also interesting. Indeed, it is at the ADF site

405   that on-site and women PM2.5 concentrations are the closest which shows that this site is the

406   most representative of the pollution exposure to women. The biggest differences are found at

407   the AWB site. As already mentioned, distance from the site to the waste burning source is more

408   important than for other sites, which explains why student concentrations are much higher than

409   on-site concentrations. At the Cotonou traffic site, measurements taken from people are also

410   higher than on site measurements. Such differences can be also explained by additional

411   pollution exposure as people move around. Note that the sampling technique may also play a

412   role in such a comparison.

413 Finally, Table 2 compares our PM2.5 results to literature data for different traffic sites in the

414 world including the same daily sampling time. It is interesting to note that our values are

415 situated at the higher end of the range of PM2.5 data observed from the other sites.

3.2 Aerosol chemical composition

3.2.1 Carbonaceous aerosol Concentrations.

3.2.1.1 EC and OC variation.

419 In Figure 8, EC values are presented by size and site for each campaign and season: wet

420 season 2015 (WS15), wet season 2016 (WS16), dry season 2016 (DS16) and dry season 2017

421 (DS17). The most striking feature is that the ADF site concentrations are always higher than at

422 the other sites in the wet seasons, whereas only slightly higher or of the same order in the dry

423 seasons. Concentrations at the traffic CT site is slightly higher than at the AT site, whereas the

424 lowest concentrations are found at the AWB site. As for PM mass, these differences are mainly

425 due to the proximity of the site to the sources, where the ADF site is much closer to the sources

426 than the AT and CT sites which are located at the first level of a building at a crossroad, and

427 the AWB site which is the farthest from the source. The strength of each source is another factor

428 which can explain EC concentration variations among the sites. High concentrations at traffic

429 sites may be explained by high EC emission factors observed for vehicles (Keita et al., 2018),

430 whereas differences between wet and dry season concentrations at the ADF sites may be

431 explained by EC emission factor variations: higher EC emission factor values are obtained for

432 moist wood combustion mostly occurring during the wet season than for dry wood combustion,

433 as mentioned previously.

434 Results of the EC size distribution are very consistent among the different sites. Whatever the

435 site and the season, higher EC concentrations are found in C and UF particles compared to F

436 particle with maximum values in UF particle as found in previous studies (Marinoni et al.,

437 2005; Xiu et al., 2015).

438 In terms of seasonal variation, our results are in agreement with long-term EC measurements

439 conducted by Djossou et al. (2018) for the same sites and period. There is no marked seasonal

440 variation for the ADF site with EC peaks in WS 2016 and DS 2017. As mentioned, wet season

441 EC peaks can be explained by the use of moist wood for cooking and smoking fish. For the

442 other sites, higher EC values are observed during the dry season rather than in the wet season

443 due to (1) decreases in EC wet deposition and concentration during the wet season and (2) the

444 influence of long-range transport from sources such as biomass burning during the dry season.

445 In terms of inter-annual variability, if we compare WS2015 and WS2016, values are slightly

446 higher in 2015 than in 2016 at the AT, CT and AWB sites. However, at the ADF site, EC

447 maximum values are observed in 2016, especially for UF particles. This is due to the source

448 which has more polluting combustion activities as previously explained. Indeed, in 2015, the

449 activities of fish and meat smoking were recent and not very well known by the population,

450 whereas they were expanded in 2016 with more workers, leading to more furnaces and

451 increased emissions.

452 EC concentrations are generally higher in DS2017 than in DS2016 for all the sites. This is not

453 due to the meteorology which is similar in both years. This is also not due to biomass burning

454 impacts. Indeed, when looking at MODIS burnt areas (http://www.aeris-

455 data.fr/redirect/MODIS-MCD64A1), burnt areas of west African savannas are higher in 2016

456 than in 2017. Therefore, EC concentrations should be higher in 2016. However, analysis of

457 back trajectories (Figure 4) reveals that biomass burning transport from northern areas are less

458 efficient in 2016 than in 2017, in both Abidjan and Cotonou. This leads to a counter effect

459 between biomass burning emission strength and air mass transport, indicating that biomass

460 burning impact could not explain the difference in EC between DS2016 and DS2017. Rather,

461 this is due to the variability of local sources. In DS2016 there was a general strike of civil

462 servants of the State with important consequences on urban activities: lower traffic and lower

463 fish smoking emissions were observed in DS2016 compared to DS2017, thus explaining the

464 lower EC concentrations at AT. Less activities were also noticed at CT.

465 OC size-speciated concentrations are presented in Figure 9 for each site and each campaign.

466 ADF OC values are always higher than at the other sites by a factor ranging from 6 to 30, for

467 all seasons and particle sizes, with highest values in DS2017. Minimum OC values are obtained

468 in DS2016. Explanations for OC variations are generally similar to the ones of EC. There are

469 less OC differences between WS2015 and WS2016 than for EC, even though WS2015 values

470 are also lower than those of WS2016, as for EC. In terms of size distribution, maximum OC

471 concentrations at the ADF site may be found in UF, then F, and finally C particles. The same

472 distribution is observed for the other sources in DS2016, however, for the other campaigns, OC

473 size distribution looks like the EC ones with higher concentrations in UF and C particles than

474 in F particles. Note that OC concentrations are higher in the CT site compared to AT for each

475 particulate size during DS, whereas during the WS, AT OC concentrations are slightly higher

476 than the CT values. This can be explained by the traffic source in each city. Indeed, the

477 consumption of petrol and diesel fuel by transport in Benin exceeds that of Côte d'Ivoire, which
478 could imply higher carbonaceous aerosol concentrations in Benin than in Abidjan in DS. In the
479 raining season, the lack of road infrastructure associated with poor road conditions prevents
480 motor vehicles from accessing certain districts in Cotonou. Traffic is thus assumed to be
481 reduced, implying lower OC concentrations in CT than in AT.
482 Table 3 compares our OC and EC values to those obtained by Djossou et al. (2018) and Xu et
483 al. (2019) for the same period and the same sites. More precisely, this comparison was done
484 between our data, Djossou's weekly data including our 3 days of measurements and Xu's daily
485 exposure data of population living closed to our sites. It is interesting to note that Djossou's
486 values are in general lower than ours. Indeed, for the wet and dry seasons, our OC
487 measurements are 4 and 1.4 times higher than Djoussou's at the AT site, 2.1 and 5.7 times
488 higher at the CT site, and 2.5 and 2.5 times higher at the ADF site, respectively. As for PM2.5,
489 this can be explained by the different sampling times between our experiments which were
490 performed at the peak of urban activities, while Djossou's dataset represents weekly integrated
491 values. Indeed, Djossou includes diurnal measurements for the whole week including lower
492 traffic activities occurring during the nighttime and the week-end period. Differences at the
493 ADF site are largely explained by the temporal pattern of fish smoking activities which take
494 place every day, only in the morning, as such the associated pollution is not well represented in
495 the weekly sampling. Finally, there are less differences at the AWB site between both datasets
496 since waste burning emissions occur night and day throughout the week. Comparisons made
497 between our values and those of Xu's personal data show that both OC and EC are of the same
498 order at the ADF site, whereas Xu values are higher than ours at the CT and AWB sites. This
499 result is in agreement with what we found with PM2.5 concentrations as detailed above.
500 Finally, Table 4 presents OC and EC for the PM2.5 comparison between our values and other
501 recent studies dealing with traffic sites in other regions of the world and with similar operational
502 conditions. We find that our values are situated in the middle of the range observed in these
503 different studies.

504 **3.2.1.2 OC to EC ratio**

505 In our study, suitable linear correlations between EC and OC are obtained in the ultrafine
506 and fine modes in all campaigns, particularly during the last one (r^2 = 0.8, 0.8, 0.9 and 0.9) at
507 the ADF, AWB, CT and AT sites, respectively. This suggests that different studied sources can
508 be assessed as significant sources of both EC and OC. As shown in Figure 10, the highest
509 OC/EC values (e.g. 25 for F particles) are obtained for WS2016 at the ADF site, whereas the

510 lowest values are found in DS2017. This is the same at all traffic sites, with ratios lower than 2

511 for DS2017. For the other campaigns, OC/EC are never higher than 5, with AT ratios slightly

512 higher than CT ratios. OC/EC ratios are more variable at the AWB site with values in 1-10

513 range. Such variations can be explained by the type of the sources characterized by different

514 OC/EC ratios, as well as by secondary aerosol organic formation which can be detected for

515 OC/EC higher than 2 (Turpin et al. 1990; Hildermann et al. 1991; Chow et al. 1996). Such a

516 process is difficult to test in our study because the sites are situated very close to the source

517 level, with the exception of the AWB site (Renjian et al. 2012). However, we find comparable

518 results between our OC/EC ratios and the one measured at the source level by Keita et al.

519 (2018). Indeed, mean OC/EC ratio measured for wood burning source by these authors is

520 approximately 11.2, which is in agreement with our data at the ADF site. In addition, OC/EC

521 ratio for the waste burning source is about 7.6, whereas our values at the AWB site are in the

522 range 2 to 10.

523 There are no marked differences between OC/EC ratios when comparing values between the

524 CT and AT sites. OC/EC ratios are globally on the same order for WS2015, WS2016 and

525 DS2016, with values similar to that of gasoline emissions or old diesel vehicle. However, the

526 ratios are lower for DS2017, with values typical of those of diesel emission (Mmari et al., 2013,

527 Keita et al., 2018). The general strike occurring in DS2016 in Abidjan could explain such a

528 difference. Indeed, more EC emissions occured in DS2017 than in DS2016 for constant OC

529 emissions. This can be the result of more diesel traffic.

530 Similar ratio values have also been previously reported for other megacities such Agra, India

531 with 6.7 (Pachauri et al., 2013), Helsinki, Finland with 2.7 (Viidanoja, 2002), Cairo, Egypt with

532 2.9 (Favez, 2008), Paris, France with 3.5 (Favez, 2008), and Milan, Italy with 6.6 (Lonati et al.,

533 2007).

3.2.1.3 Water-Soluble Organic Carbon

535 Concentrations of WSOC and WSOC/OC ratios are presented in Table 5 for each size

536 (UF, F, C and PM2.5) and campaign. As seen, WSOC are always higher at the ADF site than

537 in other sites, at least by a factor of 12. Maximum values are obtained in WS2016 with an

538 average of 16.47, 17.08 and 79.68 μgC/m³ for coarse, fine and ultra-fine fractions, respectively,

539 followed by WS2015 and DS2017. WSOC concentrations are the lowest in DS2016, with an

540 average of 4.14, 6.95 and 21.89 μg/m³ for coarse, fine and ultrafine fractions, respectively.

541 The concentrations of WSOC at the Abidjan traffic site are higher than those recorded at the

542 Cotonou traffic site in the wet seasons of 2015 and 2016, but lower in dry periods. Finally, the

543 AWB site values are on the same order as at the AT and CT sites. In terms of seasonality, there

544 is not a clear trend in WSOC values at the AWB and AT sites, whereas at the CT and ADF

545 sites, we find WSOC values to be respectively higher and lower in dry seasons compared to

546 wet seasons.

547 It is also interesting to note that WSOC are maximum in UF sizes in the AT, ADF and AWB

548 sites. At the CT site, the highest values are found in the coarse particulate fractions, except

549 during DS2016. Several factors can explain such variabilities. Firstly, WSOC concentration

550 levels are linked to meteorological factors, such as high solar radiation, which can produce

551 intense photochemical reactions and secondary organic formation (Tang et al., 2016, Favez et

552 al., 2008). Also, more WSOC may be linked to high relative humidity, but lower than 80% as

553 mentioned by Liang et al. (2016). In our study, temperatures are roughly similar in both seasons,

554 with slightly higher values in DS than in WS. This could explain the higher WSOC values

555 obtained in DS than in WS at the CT site. However, this does not explain ADF WSOC

556 variations with higher values in WS than in DS, which could be due to RH variability, higher

557 in WS than in DS. This is in agreement with Favez et al. (2008) who shows that WSOC is not

558 an adequate SOA tracer in urban environments. Secondly, WSOC concentrations can be

559 dependent on the related sources. Values at the ADF site are much higher than at other sites.

560 This is expected since wood burning is an incomplete source which is well known to produce

561 more WSOC than traffic sources (Yu et al., 2018, Tang et al., 2016, Feng 2006, Saxena and

562 Hildemann, 1996). Third, the presence of dust can produce semi-volatile organic gas

563 scavenging, and therefore WSOC and OC enhancement. Such a phenomenon can also explain

564 the highest WSOC concentrations observed in DS at the CT site where dust concentrations are

565 highest (see below paragraphs). Moreover, this can also explain why WSOC concentrations are

566 maximum in coarse particles at CT, but in ultra-fine particles at the other sites.

567 As expected, WSOC is strongly correlated with OC (r=0.7 at ADF, 0.8 at AT, 0.8 at AWB and

568 0.7 at CT), whereas correlations with EC are weaker at the AWB and CT sites with values

569 ranging from 0.1 to 0.4, respectively. The relationships between WSOC and OC and WSOC

570 and EC suggest similar primary sources and/or similar SOA formation processes. As previously

571 mentioned, source processes and characteristics explain ADF and AT values, underlining also

572 the impact of dust at the CT site. This is also confirmed by the correlation between WSOC and

573 K$^+$ at the ADF site. Finally, when looking at WSOC/OC ratios (Table 5), maximum values are

574 obtained at the ADF site with PM2.5 values as much as 43%, followed by the AT and AWB

575 sites with 32%. The lowest value (23%) is found at the CT site. The same reasons mentioned

576 earlier may explain differences in values between the ADF and other sites. However, the

577 difference between the AT and CT sites is difficult to explain since both the meteorological

578 factors and the traffic sources are similar. The only difference deals with the dust impact, higher

579 at CT than AT. It can be assumed that dust could limit WSOC formation, at high concentrations

580 or depending on sources (road dust, desert dust...). Also, Table 5 shows that there is no clear

581 seasonality in WSOC/OC values, excepted at ADF where maximum values occur during the

582 WS. Note as earlier, that ratios are maximum in ultra-fine and fine fractions for all sites except

583 at the CT site where the ratio for coarse fraction is highest.

584 Briefly, as presented in Table 6, it is interesting to compare our WSOC concentrations to

585 literature data for different traffic sites of the world. We note that our values are on the same

586 order as values found in Asia, and higher than those found in Europe.

3.2.2 Water-soluble ionic species

588 Figure 11 shows the relative contribution of the major ions to the total concentration of

589 water soluble inorganic species in the different particle modes (C, F and UF) collected at the

590 ADF, AWB, AT and CT sites for the different measurement campaigns. The concentrations of

591 different ions show significant variations from site to site. The dominant ionic species at the

592 ADF site is chloride (Cl⁻), with concentrations in the range of 2.1-12.9 µg.m⁻³, accounting for

593 18-38% of the total ions, followed by soluble potassium (K⁺), ranging from 0.9-6.6 µg.m⁻³ (8-

594 22%). The third most important element is ammonium (NH₄⁺), with concentrations in the range

595 of 1.1-5.2 µg.m⁻³ (9-15%). The mass concentrations of soluble calcium (Ca²⁺) (1.5-3.2 µg.m⁻³)

596 are on the same order of magnitude as the values for NO_3^- (0.9-3.9 µg.m⁻³), SO_4 ⁻(1.0-3.4 µg.m⁻

597 ³), and to a lesser extent, soluble sodium (Na⁺) (0.5-2.2 µg.m⁻³). However, Ca²⁺ contributions,

598 ranging from 13 to 25% of total measured ions, are higher than those of NO_3^- (7-11%), SO_4^{2-}(9-

599 11%) and Na⁺ (4-7%). The concentrations of magnesium (Mg²⁺) are low, ranging from 0.5 to

600 1.1 µg.m⁻³ (3.6-3.8%), and are as high as the sum of the remaining species (oxalic, formic and

601 acetic), constituting 2.1-7.2% of the total ion mass at the ADF site. Chloride is most likely

602 associated with sea salt origin (55% of total composition of the sea water) or secondary aerosol

603 production (Li et al., 2016). Its highest concentration at the ADF site remains lower than the

604 typical concentration in sea water, suggesting a secondary production source. The size

605 distributions of Cl⁻, K⁺, NH_4^+ and SO_4^{2-}(Figure 11a) support the conclusion that the

606 predominance of these elements in ultrafine particle mode at the ADF site could be associated

607 with anthropogenic emissions, particularly biomass combustion and domestic fires, or with

608 secondary inorganic aerosols origin. Contrarily, Ca²⁺, NO_3^- contributions to the total ions at the

609 ADF site peak mainly in the large particle fraction and may be attributed to quasi natural origin,

610   primarily to dust emissions and nitrate formation by reaction processes, respectively. In

611   addition, Na^+ and Mg^{2+} display similar size distributions at the ADF site, with the major

612   contribution in the fine particle fraction, suggesting the common sea salt origin of these two

613   elements (Belis et al., 2013).

614   NO_3^- is the major ionic component at the AWB, AT and CT sites, representing 21-36% of the

615   total water soluble inorganic concentration (i.e. 1.8-6.4 µg.m^{-3}), 12-33% (1.1-5.0 µg.m^{-3}) and

616   12-32% (1.6-7.4 µg.m^{-3}), respectively. The second major contributor is Cl$^-$, accounting for 12-

617   28% of the ion mass (1.1-2.9 µg.m^{-3}) at AWB, 6-30% (0.6-2.8 µg.m^{-3}) at AT and 7-27% (1.5-

618   4.6 µg.m^{-3}) at CT, followed by SO_4^{2-} with percentages of 9-20% (1.0-3.5 µg.m^{-3}) at AWB, 9-

619   15% (0.9-2.3 µg.m^{-3}) at AT and 11-18% (1.5-4.1 µg.m^{-3}) at CT. The proportion of Ca^{2+} is higher

620   at the CT site, representing 14-26% (2.4-6.0 µg.m^{-3}) of the bulk ion mass compared to 5-21%

621   (0.5-2.3 µg.m^{-3}) at AWB and 7-19% (1.1-1.9 µg.m^{-3}) at AT, supporting the hypothesis of the

622   high influence of re-suspended road dust by wind and motor vehicles at the Cotonou site and/or

623   long range transport of dust. Na^+ concentrations measured at the AWB, AT and CT sites are

624   slightly lower than those of Ca^{2+}, with values from 0.4 to 3.1 µg.m^{-3} (5 to 18%), while Mg^{2+}

625   contribution remains lower than 2% of the total ions at all sites. Note that organic gases

626   contributions at AT, CT and AWB is slightly lower than at ADF with values lower than 4%.

627   In contrast to the ADF site, the proportion of Cl$^-$ at the traffic sites (AT and CT) is most likely

628   dominated by coarse particles, while at the AWB site no clear trend is observed (Figures 11b-

629   d). These results suggest that Cl$^-$ at AT and CT probably originated from sea salt emissions,

630   while at AWB it produced from a mix of sources, including fuel combustion and mineral salt

631   from sources around the measurement sites. SO_4^{2-} is mainly found in ultrafine mode at the AT,

632   AWB and CT sites, with maximum relative contributions ranging from 10 to 40% of the total

633   ions. Conversely, the maximum concentrations of NO_3^- are observed in the coarse or fine

634   particle modes, constituting a percentage of between 10 and 50% at all sites. The importance

635   of ultrafine sulphates at the three sites is in-line with pollution sources of human origin

636   (Seinfield and Pandis, 1998), probably in the form of ammonium sulphate. The seasonal

637   variations of Cl$^-$, Na^+ and Mg^{2+} show that their individual contributions to total ions are

638   generally much higher in wet season than in the dry season for coarse and fine particles

639   combined (>1µm) (Figure 11). For example, the mean relative total percentages of Cl$^-$ at the

640   CT site are 27 and 24% in the wet seasons of 2015 and 2016, respectively, while these

641   percentages decrease significantly to 9 and 7% in the dry seasons of 2016 and 2017,

642   respectively. The Cl$^-$/Na$^+$ ratios in these particle sizes are 1.4 in both seasons, except at the ADF

643   site where these ratios increase slightly to 1.6 and 1.5 in wet and dry season, respectively,

644   slightly higher than the typical sea water ratio (1-1.2) (Hara et al.,2004).

645   In addition, strong correlation coefficients (0.97-0.99) between Cl⁻ and Na⁺ are obtained in

646   coarse particle sizes at all sites and in both seasons. Our analysis also shows that Cl⁻ in coarse

647   and fine fractions are highly correlated with Mg^{2+} (0.97 in wet season and 0.96 in dry season)

648   combining all sites, except at ADF for which these correlation coefficients decrease to 0.68 and

649   0.95 in the wet and dry season, respectively. As Cl⁻, Na⁺ and Mg^{2+} are associated with sea salt

650   origin or secondary aerosol production (Xiao et al., 2018), these results indicate that coarse Cl⁻

651   , Na⁺ and Mg^{2+} particles (>1µm) from this study have the same "sea salt" origin at AT, CT, and

652   C... which is different at the ADF site. Their abundance in the wet season could be related to

653   the influence of the predominant wind direction mainly oriented towards the North-East (Figure

654   5) which transports marine aerosols to these sites. Contrarily, in the ultrafine particle mode,

655   these elements have higher percentages in the dry season than in the wet season, with correlation

656   coefficients between Cl⁻ and Na⁺ (Cl⁻ and Mg^{2+}) from 0.44 (0.62) at the ADF site to 0.62 (0.70)

657   at the rest of the sites. This suggests secondary production of these very fine ions.

658   As shown in Figure 11, the relative percentage of SO_4^{2-}, NH_4^+ and NO_3^- in the different particle

659   modes is reduced in the wet season, except at the ADF site for which the proportions of

660   SO_4^{2-} and NH_4^+ tend to increase during that period, especially in the ultrafine particles. During

661   the wet season, the clean winds surrounding the ocean before reaching the measurement sites

662   (Figure 5, top) could contribute to lower the proportion of these species, in addition to the

663   scavenging processes during the rainy season. Unlike the wet season, a relatively good

664   correlation of 0.87 (SO_4^{2-} versus NH₄⁺), 0.73 (NO_3^- versus NH₄⁺) and 0.87 (SO_4^{2-} versus NO_3^-)

665   has been found in coarse particles (>1µm), indicating similar sources for these three species

666   during the dry season. In order to try to identify these sources, the ratio of SO_4^{2-}/Ca^{2+} and

667   NO_3^-/Ca^{2+} has been determined. The average SO_4^{2-}/Ca^{2+} and NO_3^-/Ca^{2+} ratios in combined

668   coarse and fine particles at all sites except ADF (1.07 and 2.58 during the wet season and 0.33

669   and 1.60 during the dry season) are higher than the corresponding ratios for soil (0.026 and

670   0.003, respectively). On the other hand, the SO_4^{2-}/Ca^{2+} ratio increases in the ultrafine particles

671   (5.07 during the wet season and 2.53 during the dry season), while that of NO_3^-/Ca^{2+} remains

672   almost constant (2.86 during the wet season and 1.65 during the dry season). This implies that

673   the atmosphere around the AWB, AT and CT sites is enriched by SO_4^{2-} formed as

674   anthropogenic secondary particles, possibly from sulfur containing sources, particularly in

675   ultrafine particle mode, and by NO_3^- mostly coming from nitrogen containing sources in all

676   particle sizes. The higher contributions of these elements during the dry season could result

677   from a combination of several factors: 1) an atmosphere loaded with dust favoring

678   heterogeneous chemistry to obtain secondary aerosol and the rise of biomass burning emissions;

679   2) the increase of photochemical activity and higher concentrations of hydroxyl radicals in the

680   dry season, which can oxidize SO_2 from biomass combustion (Arndt et al., 1997) to SO_4^{2-} (Li

681   et al., 2014) ; and 3) the wind transport of anthropogenic secondary particles from the industrial

682   zone located upstream from our sites. As previously shown, maximum values of SO_4^{2-}, NH_4^+

683   and NO_3^- observed during the wet season the ADF site may be linked to anthropogenic

684   emissions, and more precisely smoking activities which pollute more in the wet than dry season.

685   **3.2.3. Elemental concentrations**

686   Table 7 shows the mean values of the major metallic elements of total particulate matter

687   at the different studied sites for the wet season 2016 and dry season 2017. Note that data of

688   elemental concentrations are not available for the wet season 2015 or dry season 2016. In

689   addition, only bulk metal concentrations and their corresponding relative abundances are

690   examined. As shown in Table 7, the concentrations of metal elements span a wide range, from

691   0.2 to 25.2 µg.m^{-3}. Among the measured elements, Al, Na and Ca are the most abundant,

692   followed by Fe, K and Mg. The percentage of Al accounts for 13.7% of the total re-suspended

693   particles in the dry season 2017 (3.5% in the wet season 2016) at the AWB site, 12.3% (2.4%)

694   at the AT site, 1.8% (0.4%) at the ADF site and 5.7% (4.4%) at the CT site, while that of Na

695   represents 12.8% (6.6%) at the AWB site, 13.4 (3.1%) at the AT site, 1.2 (0.6%) at the ADF

696   site and 4.3 (5.8%) at the CT site. Ca contributes to 1.6% (0.8%) of the total PM mass at the

697   AWB site, 3.6% (0.4%) at the AT site, 0.8% (1.1%) at the ADF site and 2.3% (5.4%) at the CT

698   site. These major three elements (Al, Na and Ca) together have concentrations in the wet season

699   2016 (dry season 2017) of 6.2 (51.5) µg.m^{-3}, 5.4 (33.5) µg.m^{-3}, 14.3 (33.2) µg.m^{-3} and 7.6 (21.2)

700   µg.m^{-3}, accounting for 11.0% (28.1), 5.9% (29.3), 15.5% (12.3) and 2.0% (3.8) of the total PM

701   mass at the AWB, AT, CT and ADF sites, respectively. The absolute (and relative) abundances

702   of Fe, K and Mg combined are 1.5 µg.m^{-3} (2.6%) in the wet season and 10.3 µg.m^{-3} (5.6%) in

703   the dry season at the AWB site. These values are 1.5 µg.m^{-3} (1.7%) and 5.7 µg.m^{-3} (5.0%) at

704   AT, 3.2 µg.m^{-3} (3.5%) and 9.3 µg.m^{-3} (3.4%) at CT and 3.9 µg.m^{-3} (1.1%) and 12.3 µg.m^{-3}

705   (2.2%) at ADF. The highest metal concentrations are generally measured during the dry season

706   2017 at all sites, except at CT where relatively similar values are obtained for the two seasons.

707   The seasonal variability in all the mentioned traces elements may be attributed to drier

708   conditions during the dry season (Figure 4) in West Africa favoring dust particle re-suspensions.

709 In addition, the dry season in West Africa is marked by the Harmattan continental winds

710 bringing dust from the Saharan desert (Figure 5). Moreover, it is interesting to note that the lack

711 of seasonal variability at CT may be due to the much poorer road conditions found at Cotonou

712 compared to Abidjan.

713 Most all of these elements are generally considered to have natural origins such as the earth's

714 crustal dust and sea salt (Al-Momani, 2003). However, K can also be associated with biomass

715 burning (De Oliveira Alves et al., 2015). As previously mentioned, the seasonal cycle of Fe, K

716 and Mg together suggests contributions to the bulk mass which are about twice as high in the

717 dry season than in the wet season at all measurement sites. This trend is driven by the large

718 variability of the element K which shows percentages in the dry season 4 to 10 times higher

719 than those in the wet season, likely due to more biomass burning activity during the winter time.

720 The other metals (Ti, P, Zr, Zn, Cr, Mn, Pb and Ni) represent less than 0.5% and 2% in the wet

721 and dry seasons, respectively, at all sites, with Cr, Mn, Pb and Ni exhibiting less seasonal

722 variability compared to the rest of the metal elements. The low proportions of these non-crustal

723 elements in the studied sites suggest a small contribution of elements primarily emitted by

724 anthropogenic activities such as industrial processes (Viana et al., 2007; Viana et al., 2008;

725 Minguillón et al., 2014).

726 The highest contribution of metal elements is obtained at the AWB and AT sites, reaching 35.8

727 and 35.2% of the total PM mass in the dry season, respectively. These maximum percentages

728 are due to the large contribution of both Al and Na crustal elements which account for about

729 26%. The lower proportion of metal elements at the ADF site (6.5% of the bulk concentration)

730 can be explained by the less dominant influence of re-suspended dust particles compared to

731 domestic fire sources. At the CT site, all elemental concentrations contribute to 16.3 % of total

732 PM for the dry season. However, during the wet season, the highest metal contribution of 19.5%

733 is obtained at CT, followed by AWB (14%) and AT (8.2%). The value at ADF remains the

734 lowest (3.3%). Again, the maximum percentage at the CT site is a result of the fact that most

735 of the roads in Cotonou are unpaved, therefore particle resuspension occurs in all seasons.

736 To assess the relative contribution of crustal and non-crustal to elemental aerosol loadings,

737 source enrichment factor (EF), as well as elemental ratios, are often used as diagnostic tools

738 (Weckwerth, 2001; Voutsa et al., 2002). EF are calculated using both literature data of the

739 typical elemental composition of the upper continental crust (Mason and Moore, 1982; Taylor,

740 1964) and measured metal composition from this study. Using Al as a reference element, the

741 EF of an atmospheric element X is calculated using the following formula:

$$\mathrm{EF_X} = \frac{\frac{[X]_{atm}}{[Al]_{atm}}}{[X]_{soil} \big/ [Al]_{soil}}$$

742

743 Where $[X]_{atm}$ and $[Al]_{atm}$ are the concentrations of the chemical element X and Al in the

744 atmosphere, respectively, and $[X]_{soil}$ and $[Al]_{soil}$ are the typical concentrations of the element

745 X and Al in the earth's crust, respectively. Al is frequently used as a reference element assuming

746 that its anthropogenic sources in the atmosphere are negligible (Gao et al., 2002; Cao et al.,

747 2005; Xu et al., 2012). From the EF values, source contributions are estimated following the

748 method described by Arditsoglou and Samara (2005). Note that these studies only refer to ratios

749 for a limited list of sources. Incomplete diagnostic may be expected due to the African source

750 specificities focused on here. Also, note that the literature data are sometimes different for the

751 same source.

752 In all sampling sites, EF values typically lower than 5 are obtained for several trace elements

753 (Be, Sc, Ti, V, Fe, Ga, Sr, Nb, Rh, Ba, La, Ce, Pr, Nd, Sm, Eu, Gd, Tb, Dy, Ho, Er, Tm, Yb,

754 Lu, Ta, Th, U). This suggests natural origin of these species and therefore a negligible

755 contribution of anthropogenic emissions (Freitas et al., 2007; Gao et al., 2002). The most

756 enriched elements (EF>100) are Sb, Sn, Zn, Se, Te, Cd, Pb, Bi and Mo at nearly all of the sites,

757 indicating significant anthropogenic origin (Wang et al., 2006). These elements are mainly

758 emitted into the atmosphere through fossil fuel combustion, traffic emission, wear of brake

759 lining materials and industrial processes (Watson and Chow, 2001; Samara and al., 2003).

760 Different elemental ratios have been used as diagnostic tools to identify sources of atmospheric

761 particles, including Cu/Sb, As/V, V/Ni, Zn/Pb and Zn/Cd (Weckwerth, 2001; Samara et al.,

762 2003; Herut et al., 2001; Foltescu et al., 1996; Arditsoglou and Samara, 2005. As mentioned,

763 incomplete diagnostic is expected and the literature values can be different for the same source.

764 The mean values of selected elemental ratios in TSP from the Abidjan (ADF, AWB and AT)

765 and Cotonou (CT) sites are presented in Table 8. The Cu/Sb ratio is proposed as a good indicator

766 for brake lining wear (Weckwerth, 2001; Sternbeck et al., 2002) and, consequently, as a tracer

767 for traffic sources. Weckwerth (2001) and Sternbeck et al. (2002) reported a Cu/Sb ratio close

768 to 5 as a diagnostic criteria for brake wear particles in the ambient air. In this study, very low

769 ratios of 0.28±0.21 in the wet season 2016 and 0.56±0.21 in the dry season 2017 are found at

770 the ADF site. Relatively similar values are obtained at the CT site (0.57 in the wet season and

771 0.19±0.16 in the dry season). These ratios are on the same order of magnitude as those typical

772 for soil (0.3) (Watson et al. 2001). At both the AWB and AT sites, Cu/Sb ratios ranging between

773 0.01 and 0.16 are obtained in the dry season 2017, which seems to also indicate an influence of

774   re-suspended particles at these two sites during that period. In the other three sites (ADF, AT

775   and CT), however highly influenced by traffic, our Cu/Sb ratios do not compare with brake

776   lining wear ratios, but rather with soil ratios only. In contrast, very high and large ranges of

777   ratios varying from 238.7 to 3725.9 are calculated at the AWB site during the wet season 2016.

778   Arditsoglou and Samara (2005) proposed a Cu/Sb ratio of 700 as a tracer of diesel vehicle

779   emissions. Here high values could be also be explained by waste burning materials, values

780   which are not known in literature to our knowledge

781   Typically, an As/V ratio of 0.02 indicates that the emissions are from burning oil, 0.03 for

782   cement plan, 0.1 for soil or agricultural soil, 0.3 for metal scrap incineration source and 2.3 for

783   petrol and diesel origin (Lee et al., 2000; Watson and Chow, 2001; Samara et al., 2003). The

784   aerosols in Abidjan have an As/V ratio ranging from 0.28 to 0.95 during the dry season 2017,

785   implying an anthropogenic origin for As, including petrol and diesel vehicles. Only one value

786   of 0.07, four times lower than the lower limit of the As/V ratio found in the dry season, is

787   present in Abidjan during the wet season. This is not enough to determine a possible seasonal

788   variation of the ratio As/V in Abidjan. However, in Cotonou, similar As/V ratios (0.15±0.19 in

789   the wet season and 0.15±0.06 in the dry season) are observed for both seasons, and these values

790   remain lower than those from Abidjan. This result suggests more dust origin for As in Cotonou.

791   This is in-line with values reported in the literature: Watson et al. (2001) and Lee et al. (2000)

792   reported a ratio of 0.1 as tracer of soil or agricultural soil.

793   The V and Ni trace elements are frequently used as fingerprint makers for petroleum derived

794   hydrocarbons (Laden et al., 2000). The V/Ni ratio for oil combustion has been reported to range

795   from 2 to 5 (Foner and Ganor, 1992; Almeida et al., 2005; Arditsoglou and Samara, 2005),

796   while that of vehicle emissions are generally lower than 2 (0.15 for diesel, 0.4 for a mixture

797   gasoline and diesel, 0.02 for gasoline, Samara et al., 2005; Watson and Chow, 2001). In

798   Abidjan, the average ratio of V/Ni is 0.17±0.11 at ADF, 0.20±0.20 at AWB and 0.22±0.11 at

799   AT with ratios in the dry season higher than those in the wet season, except at the AT site for

800   which the ratio is slightly larger during the wet period (Table 4). In Cotonou, the V/Ni ratio is

801   relatively higher than in Abidjan, varying from 0.13 to 0.66, with values in the wet period 1.4

802   times larger than during the dry season (Table 8). These results suggest that oil combustion is

803   a minor source of Ni and V in both Abidjan and Cotonou, which is due to the absence of

804   industrial pollution from the combustion of heavy-fuel oil. On another hand, these low Ni/V

805   ratios seem to support the assumption of the strong influence of vehicle emission sources on all

806   studied sites.

807 The ratio of Zn/Pb has been used to distinguish between transported and local aerosols. From

808 this study, ranges of the Zn/Pb ratio (1.8-8.2 at ADF, 3.6-17.4 at AWB, 8.3-25.5 at AT and 3.5-

809 22.5 at CT site) are representative of the ratios found for gasoline and diesel vehicles (1.7-2.4,

810 Qin et al., 1997 ; Sakata et al., 2000 ; Watson et al., 2001 ; Chiang et al., 2012), for roadside

811 (4.2-4.4, Zhang et al., 2018), for soil and agricultural soil (3.1-4.0, Watson et al., 2001 ; Lee et

812 al., 2000), for earth's crust and road dust (5.4-5.5, Mason and Moore, 1982 ; Shen et al., 2016),

813 for biomass burning and metal scrap incineration (7.2-8.4, Lee et al., 2000 ; Samara et al., 2003)

814 and combustion of petrol oil from road transport (10.6-24.4, Pulles et al., 2012). Zn/Pb ratios

815 calculated at both the ADF and AT sites during the dry season (2.8±1.3 and 14.8±3.8,

816 respectively) are lower than those observed during the wet season (7.1±3.4 and 19.9±14.7,

817 respectively), while at Cotonou a lower Zn/Pb ratio is found during the wet period (3.3±2.3)

818 compared to the dry period (18.5±8.5). This seasonal variation of the ratio Zn/Pb suggests that

819 TSP in Abidjan is more affected by local emissions during dry season, while aerosols in

820 Cotonou are more influenced by transported and re-suspended dust, which is in agreement with

821 our previous conclusions. Also it is important to note that the mean values found at AT and CT

822 (on the order of 18) are indicative of combustion of petrol from road transport origin (Pulles et

823 al., 2012), whereas that of the ADF site (7.1) could suggest possible links to biomass burning

824 (Samara et al., 2003).

825 Finally, the Zn/Cd ratio has been also examined. A value of 29 close to ratio reported for

826 gasoline vehicle (27, Qin et al., 1997) is obtained for the ADF site, indicating that this site is

827 also impacted by traffic sources. A values of 56 is obtained for the AWB site which is in close

828 agreement with values reported for oil burning (Watson et al., 2001, Samara et al., 2003). That

829 could indicate that oil might be one of the waste burning materials.

830 ### 3.2.4 Dust

831 As shown in the methodology part and in the previous paragraph, we can see that desert

832 dust and parent soils are mainly composed of clays, feldspar, and quartz, therefore contain high

833 contents of silicon, aluminium, calcium and iron (Schütz and Rahn 1982; Laurent, 2005), the

834 main elements from which dust concentrations are obtained. Figure 12 shows dust

835 concentrations calculated from Ca^{++} values following the Sciare et al. (2005) relationship (see

836 paragraph 2.3.6) for Coarse (C), Fine (F) and UltraFine (UF) particle sizes at the different sites

837 for each season. Note that no UF value exists for the wet season 2016 due to our sampling

838 procedure at this time.

839 During the wet season, the average total concentrations range from 5.2 to 25.2 µg.m^{-3} in 2015

840 and 13.5 to 43.0 µg.m^{-3} in 2016, with slightly higher values at the CT and ADF sites, whereas

841 during the dry season, values range from 16.8 to 66.2 µg.m^{-3} in 2016 and from 17.6 to 61.3

842 µg.m^{-3} in 2017, with maximum concentrations obtained at the CT site. When considering mean

843 values of the wet and dry seasons respectively, total dust at Cotonou traffic (CT) are 2.2 and

844 3.1 times the values found at AT, 4.4 and 2.9 times at AWB and 1.2 and 3.1 times at ADF.

845 Seasonal comparison shows that mean dust concentration are higher in the dry seasons than in

846 WS 2015 by a factor of 1.1 for ADF, 1.8 for AT, 2.5 for CT and 4.1 for AWB. A striking feature

847 is that wet season 2016 presents higher values by a factor of 1.6 to 2.6 than wet season 2015.

848 Also, it is interesting to note that the dust content in coarse particles is higher in DS2017 than

849 in DS2016. Moreover, dust is maximum for coarse particles during the wet season 2016,

850 whereas for fine and ultrafine particles during the dry seasons and the wet season 2015. Such

851 variations may be explained by different factors: road dust resuspension processes, long range

852 transport of desert dust from Bodélé depression in Tchad (Prospero et al., 2002; Washington et

853 al., 2003; Knippertz et al., 2011) and/or from northern dusty countries (Mali, Niger) (Ozer,

854 2005) by northerly winds in dry season (Balarabe et al., 2016), and meteorological factors such

855 as wind intensity and direction, and precipitation. It is important to note that the latter factor

856 does not explain any trends since precipitation and wind are similar between the two wet

857 seasons. We recall that the long-range transport of dust occurs at low elevations during the dry

858 season, and often at higher altitudes during the rest of the year following the northward

859 movement of the intertropical front (Afeti and Resch , 2000; Middleton et al., 2001). To go

860 further in our analysis, AOD at 550nm from MODIS satellite images (http://www.aeris-

861 data.fr/redirect/MODIS-MCD64A1) associated with back trajectories (Figure 4) were

862 examined for each date of our intensive campaigns in Abidjan and Cotonou. No clear

863 indications are found since images do not cover our area for all periods. The interesting pattern

864 shown in Figure 13 is the AOD difference between Cotonou and Abidjan for DS2017, with

865 higher values at Cotonou than in Abidjan for the campaign period, likely because dust events

866 have a larger impact in Benin than Côte d'Ivoire. This is confirmed by the DACCIWA

867 sunphotometer AOD and Angström coefficient (AE) measurements at Abidjan and Cotonou

868 (Léon et al., 2019; Djossou et al., 2018). Indeed, in DS2017, during our period of

869 measurements, mean AOD in Cotonou is of the order of 1.3 versus 0.9 in Abidjan for an AE of

870 0.6 for both sites, which clearly indicates the presence of coarse dust particles. Also, when

871 comparing DS2016 and DS2017 at Cotonou, we can see that lower AOD values (mean: 0.99)

872 with higher AE values (mean: 1.1) are observed. This is in agreement with the increase of dust

873   concentrations in the coarse fraction observed between 2016 and 2017 shown in Figure 12. If

874   we focus now on the two wet seasons, as mentioned earlier, dust concentrations are much higher

875   in 2016 than in 2015 at the CT and ADF sites. It is consistent with observed AOD values at CT

876   which increased by a factor of 2 between 2015 and 2016. No AOD value is given by Léon et

877   al. (2019) at Abidjan in WS2015 to allow such comparison in Abidjan. Moreover, during the

878   WS, an AE on the order of 1 may be found at CT, indicating smaller particles which could be

879   due to road resuspension. It is interesting to note that during WS 2016, AOD and AE are

880   respectively higher and lower at Abidjan than at Cotonou. Again, this is consistent with our

881   dust concentrations at CT. In Abidjan, we could assume that another source of Ca^{++}, which is

882   not taken into account in our dust calculations, may explain our dust concentration data. That

883   may be the result of anthropogenic Ca^{++} emissions from residential combustion, more important

884   in 2016 than in 2015 as shown earlier

885   (http://naei.beis.gov.uk/overview/pollutants?pollutant_id=84).

886   **3.3 Aerosol chemical closure**

887   The aerosol chemical closure obtained using the Guinot et al. (2007) method (see below)

888   at the different sites for each season is presented in Figure 14. Results show clear intra- and

889   inter-annual variations at all of the sites, as well as significant differences among the sites. In

890   total, dust accounts for 25 to 60% of the bulk PM mass (depending on the measurement

891   campaign) at both traffic sites, with no clear seasonal cycle for the year 2016, and higher

892   contributions in Cotonou (Figures 14c and 14d). These percentages vary from 30 to 65% at the

893   AWB site, and from 10 to 30% at the ADF site, with percentages 1.5 and 2 times higher in the

894   dry season than in the wet season for the year 2016 (Figures 14a and 14b). This high

895   contribution is related to the Saharan dust transport occurring during the dry season as

896   demonstrated earlier. The largest percentage observed in Cotonou can be explained by the

897   influence of local dust, mainly from unpaved roads (only 8% of roads are paved compared to

898   59.4% in Abidjan (UVICOCI, 2018)). The relative contribution of dust generally peaks in the

899   coarse mode and, to a lesser extent, in the fine mode, at all sites considered, reflecting their

900   natural origin. However, the dust contribution in the ultrafine mode remains important. It is

901   interesting to note that the dust contribution observed in this study for the year 2016 at the

902   Abidjan sites is in agreement with the results of Xu et al. (2019) which show a PM2.5 dust

903   contribution of 35-50% compared to our values of 18-52%.

904   Carbonaceous aerosol, the sum of EC and POM, show large contributions at the ADF site (up

905   to 75% of the total PM mass), with relatively similar proportions in each season (Figure 14a).

906   The absence of a clear seasonal pattern is also observed at the other sites, except at AWB where

907   carbonaceous aerosol contributes to 35% of the bulk PM mass in the wet season, and 15% in

908   the dry season of 2016 (Figures 14b-d). However, carbonaceous aerosol contribution accounts

909   for about 18-25% of the total mass at both traffic sites. As seen in Figure 14, in most of the

910   cases, carbonaceous aerosol contribution sharply increases from the coarse to ultrafine mode in

911   all sites during both seasons, with the exception of the ADF site during the wet season 2015.

912   As shown previously, the importance of carbonaceous aerosol at the ADF site reveals, on one

913   hand, the proximity between active sources such as domestic fires and the sampling site, and

914   on the other hand, the specificity of the site characterized by lots of wood burning activities.

915   These activities are responsible of high incomplete combustions with high emission factor

916   values (Keita et al., 2018). In addition, as an indicator of incomplete source, the EC-to-POM

917   ratio obtained for the ADF site is 3 to 4 times lower than the values calculated for the other sites

918   (Figure 14).

919   The average total concentrations of ionic species are 27.4 $\mu g.m^{-3}$ in the wet season (19.0 $\mu g.m^{-3}$

920   in the dry season), 12.5 (11.3 $\mu g.m^{-3}$), 13.2 (7.8 $\mu g.m^{-3}$) and 14.8 (17.3 $\mu g.m^{-3}$) at the ADF,

921   AWB, AT and CT sites, accounting for 5.7 (5.4%), 19.2 (6.5%), 14.7 (5.7%) and 14.4 (6.4%)

922   of bulk PM, respectively. The percentages of the total WSI to PM mass (15-20%) at the three

923   Abidjan sites (ADF, AWB and AT) are on the same order of magnitude than the data from

924   PM2.5 personal exposure samples collected at the same locations in 2016 by Xu et al. (2019).

925   Our results also are very close to the ionic contribution of 9% of the PM10 mass found at the

926   urban curbside site in Dar es Salaam in Tanzanie during the wet season 2005 by Mkoma (2008).

927   Our results indicate no clear seasonal cycle. The highest WSI concentration during the wet

928   season at both sites can be explained by the impact of marine aerosols during this season. In

929   addition, at the ADF site, the large use of moist wood for cooking can play a role. At the CT

930   site, and to a lesser extent at AWB site, WSI concentrations are almost constant in the two

931   seasons, indicating that WSI originates more from anthropogenic than natural sources.

932   The ion percentages of C, F and UF PM fractions are 4.8, 6.1 and 10.4% for ADF, 13.7, 24.9

933   and 22.8% for AWB, 11.5, 24.7 and 12.4% for AT and 12.4, 26.3, 13.0% for CT, respectively,

934   indicating higher values in fine mode except at ADF where the contribution is largest for the

935   UF mode (Figure 14). These results suggest that WSI at the ADF site are from direct

936   anthropogenic emissions, while at the rest of the sites they originate from fresh marine aerosols.

937

4- Conclusions

938

939 This paper presents the mass and the size-speciated chemical composition of particulate matter

940 (PM) during the dry and wet seasons in Abidjan and Cotonou. Measurements were performed

941 at three sites in Abidjan, representative of domestic fire (ADF), waste burning (AWB) and

942 traffic (AT) sources, and at one traffic site in Cotonou (CT). The total PM mass concentrations

943 show large variabilities (56-676 µg.m^{-3}) and a clear seasonality with concentrations in the dry

944 season 1.5 to 3 times higher than those in the wet season, except at the ADF site where values

945 in the wet period are larger. The ADF site is the most polluted site and a significant fraction of

946 the aerosol mass is in ultrafine (UF) and fine (F) particle modes, which can have the largest

947 impact on the respiratory tract. It is interesting to note that all these values are well above the

948 WHO guideline of 25 µg/m^3, irrespective of season and size. This is a warning signal for

949 pollution levels in African capitals if nothing is done to reduce emissions in the future. The

950 analysis of chemical species indicates a predominance of particulate organic matter (POM) at

951 the ADF site, especially in the UF and C fractions, while at CT, dust particles are the major

952 constituent. The specificity of the ADF site is likely related to the presence of burning activities

953 where women dry fish and meat using wood before selling them. In the wet season, the wood

954 is moist and combustion is highly incomplete, producing a lot of smoke and much higher

955 aerosol concentrations than in the dry season. The large contribution of dust to the African

956 aerosols results from road dust resuspension processes, and the long-range transport of desert

957 dust associated with the Bodélé depression. The largest percentage observed at Cotonou may

958 be explained by the more predominant influence of local dust, mainly from unpaved roads (only

959 8% of roads are paved, compared to 59.4% in Abidjan). The comparison of traffic sites reveals

960 that concentrations at the CT site are higher than those at AT. This can be explained not only

961 by the strong influence of dust in Cotonou, but also by the consumption of petrol and diesel

962 fuel by transport which exceeds the one of Abidjan. The carbonaceous aerosols generally peak

963 in the UF and F particle modes. This is likely associated with anthropogenic emissions,

964 particularly biomass and waste combustion, domestic fires and traffic.

965 Results from the chemical closure indicate clear seasonal and inter-annual variability within the

966 same site, as well as significant differences between the sites. In total, dust accounts for 25 to

967 60% of the bulk PM mass at both traffic sites, with no clear seasonal cycle for the year 2016,

968 and higher contribution at Cotonou. These percentages vary from 30 to 65% at the AWB site

969 and from 10 to 30% at the ADF site. The relative contribution of dust generally peaks in the

970   coarse mode, and to a lesser extent, in the fine mode for all sites, reflecting their natural origin.

971   Nevertheless, the dust contribution in the ultrafine mode remains important.

972   Carbonaceous aerosol, the sum of EC and POM, shows large contributions at the ADF site (up

973   to 75% of the total PM mass), with relatively similar proportions in each season. The absence

974   of seasonality is also observed at the other sites, except at AWB where carbonaceous aerosol

975   contributes to about 35% of the bulk PM mass in the wet season and 15% in the dry season of

976   2016. However, based on 2016, carbonaceous aerosol accounts for about 18-25% of the total

977   mass at both traffic sites. In most cases, the carbonaceous aerosol contribution sharply increases

978   from coarse to ultrafine mode for all sites and seasons, except at the ADF site during the wet

979   season 2015. This result is consistent with previous studies showing that carbonaceous aerosol

980   generally peaks in the fine mode due to their anthropogenic origin. The importance of

981   carbonaceous aerosol at the ADF site reveals both the proximity between the active sources

982   such as domestic fires to the sampling site, as well as the specificity of the site characterized by

983   intense wood burning activities, which lead to high incomplete combustions. In addition, as an

984   indicator of incomplete source, the EC-to-POM ratio obtained at the ADF site is 3 to 4 times

985   lower than the values calculated at the other sites.

986   The average total concentrations of ionic species are 27.4 $\mu g.m^{-3}$ in the wet season

987   (19.0 $\mu g.m^{-3}$ in the dry season), 12.5 (11.3 $\mu g.m^{-3}$), 13.2 (7.8 $\mu g.m^{-3}$) and 14.8 (17.3 $\mu g.m^{-3}$) at

988   the ADF, AWB, AT and CT sites, accounting for 5.7 (5.4%), 19.2 (6.5%), 14.7 (5.7%) and 14.4

989   (6.4%) of the bulk PM, respectively. At the ADF site, maximum values of SO_4^{2-}, NH_4^+ and

990   NO_3^- observed during the wet season may be linked to the impact of anthropogenic emissions

991   and, more precisely, to smoking activities which pollute more in the wet than in the dry season.

992   However, our results indicate no clear seasonal cycle for WSI. The higher WSI concentration

993   during the wet season at the other sites can be explained by the impact of marine aerosols during

994   this season.

995   The WSI percentages in C, F and UF PM fractions for the ADF, AWB, AT and CT sites,

996   respectively, indicate a peak in the fine mode except at ADF where the contribution is largest

997   in the UF mode. These results confirm that WSI at ADF is due to anthropogenic emissions. In

998   terms of trace elements, they present a well-marked seasonal evolution. The highest

999   concentrations registered during the dry season are for the Al specie, followed by Fe. The mean

1000   values of selected trace element ratios in TSP for the Abidjan (ADF, AWB and AT) and

1001   Cotonou (CT) sites indicate the influence of dust particles at these sites during that period. At

1002   the ADF, AT and CT sites, As/V ratios from 0.28 to 0.95 in DS2017, indicate the anthropogenic

1003   origin of As, especially from petrol and diesel vehicles. The seasonal variation of the Zn/Pb

1004 ratio suggests that TSP in Abidjan is more affected by local emissions during the dry season,
1005 while Cotonou aerosols are more influenced by transported and re-suspended dust, which is in
1006 agreement with our previous conclusions. Finally, the Zn/Cd ratio has been also examined, with
1007 a value of 29 at the ADF site. This indicates that the ADF site is also impacted by traffic sources.
1008 Finally, WSOC concentrations for each site, size and season have also been evaluated. It is
1009 interesting to note that such values are maximum at the ADF site for the wet season. At this
1010 site, the WSOC/OC and WSOC/K ratios highlight the primary origin of WSOC due domestic
1011 fire emissions. We also note the high concentrations of WSOC at CT in the dry season which
1012 is related to large dust concentrations and heterogeneous chemistry.

1013 Our study constitutes an original database to characterize urban air pollution from
1014 specific African combustion sources. The next step will be to cross such an exhaustive aerosol
1015 chemical characterization to biological data in order to evaluate the impact of aerosol size and
1016 chemical composition on aerosol inflammatory properties.

1017

1018 **Acknowledgements**. The research leading to these results has received funding from the
1019 European Union 7th Framework Programme (FP7/2007-2013) under Grant Agreement no.
1020 603502 (EU project DACCIWA: Dynamics-aerosol-chemistry-cloud interactions in West
1021 Africa). The authors greatly thank all the colleagues and operators who contribute to sampling
1022 during the different campaigns.

1023

1024 **Author Contributions**

1025 J.A. and C.L. conceived and designed the study. J.A., C.L. and T.D. contributed to the
1026 literature search, data analysis/interpretation and manuscript writing. J.A., C.L., A.B., TD. and.
1027 contributed to manuscript revision. J.A., C.L., J.F.L, H.C, V.Y., A.A, C.G, C.Z, E.C and S.K.
1028 carried out the particulate samples collection and chemical experiments, analyzed the
1029 experimental data.

1030 **Additional Information**

1031 Fig. S1 and Appendix A-D accompany this manuscript can be found in Supplementary
1032 Information.

1033 **Competing financial interests**

1034 The authors declare no competing financial interests

1035

1036 **References**

Adon, M., Galy-Lacaux, C., Yoboué, V., Delon, C., Lacaux, J. P., Castera, P., Gardrat, E., Pienaar, J., Al Ourabi, H., Laouali, D., Diop, B., Sigha-Nkamdjou, L., Akpo, A., Tathy, J. P., Lavenu, F. and Mougin, E.: Long term measurements of sulfur dioxide, nitrogen dioxide, ammonia, nitric acid and ozone in Africa using passive samplers, Atmos. Chem. Phys., 10(15), 7467–7487, doi:10.5194/acp-10-7467-2010, 2010.

Afeti, G. M. and Resch, F. J.: Physical characteristics of Saharan dust near the Gulf of Guinea, Atmospheric Environment, 34(8), 1273–1279, doi:10.1016/S1352-2310(99)00296-4, 2000.

Alastuey, A., Querol, X., Castillo, S., Escudero, M., Avila, A., Cuevas, E., Torres, C., Romero, P., Exposito, F. and Garcia, O.: Characterisation of TSP and PM2.5 at Izaña and Sta. Cruz de Tenerife (Canary Islands, Spain) during a Saharan Dust Episode (July 2002), Atmospheric Environment, 39(26), 4715–4728, doi: 10.1016/j.atmosenv.2005.04.018, 2005.

Almeida, S., Pio, C., Freitas, M., Reis, M. and Trancoso, M.: Source apportionment of fine and coarse particulate matter in a sub-urban area at the Western European Coast, Atmospheric Environment, 39(17), 3127–3138, doi: 10.1016/j.atmosenv.2005.01.048, 2005.

Al-Momani, I.: Trace elements in atmospheric precipitation at Northern Jordan measured by ICP-MS: acidity and possible sources, Atmospheric Environment, 37(32), 4507–4515, doi: 10.1016/S1352-2310(03)00562-4, 2003.

Arditsoglou, A. and Samara, C.: Levels of total suspended particulate matter and major trace elements in Kosovo: a source identification and apportionment study, Chemosphere, 59(5), 669–678, doi: 10.1016/j.chemosphere.2004.10.056, 2005.

Arndt, R. L., Carmichael, G. R., Streets, D. G. and Bhatti, N.: Sulfur dioxide emissions and sectorial contributions to sulfur deposition in Asia, Atmospheric Environment, 31(10), 1553–1572, doi: 10.1016/S1352-2310(96)00236-1, 1997.

Avogbe, P. H., Ayi-Fanou, L., Cachon, B., Chabi, N., Debende, A., Dewaele, D., Aissi, F., Cazier, F. and Sanni, A.: Hematological changes among Beninese motor-bike taxi drivers exposed to benzene by urban air pollution, African Journal of Environmental Science and Technology, 5(7), 464-472–472, 2011.

Balarabe, M., Abdullah, K. and Nawawi, M.: Seasonal Variations of Aerosol Optical Properties and Identification of Different Aerosol Types Based on AERONET Data over Sub-Sahara West-Africa, ACS, 06(01), 13–28, doi:10.4236/acs.2016.61002, 2016.

Belis, C. A., Karagulian, F., Larsen, B. R. and Hopke, P. K.: Critical review and meta-analysis of ambient particulate matter source apportionment using receptor models in Europe, Atmospheric Environment, 69, 94–108, doi: 10.1016/j.atmosenv.2012.11.009, 2013.

Besombes, J.-L., Maître, A., Patissier, O., Marchand, N., Chevron, N., Stoklov, M. and Masclet, P.: Particulate PAHs observed in the surrounding of a municipal incinerator, Atmospheric Environment, 35(35), 6093–6104, doi: 10.1016/S1352-2310(01)00399-5, 2001.

Bisht, D.S., Dumka, U.C., Kaskaoutis, D.G., Pipal, A.S., Srivastava, A. K., Soni, V.K., Attri, S.D., Sateesh, M., Tiwari, S.: Carbonaceous aerosols and pollutants over Delhi urban environment: Temporal evolution, source apportionment and radiative forcing, Science of the Total Environment., 521-522: 431-445, 2015a.

Bouhila, Z., Mouzai, M., Azli, T., Nedjar, A., Mazouzi, C., Zergoug, Z., Boukhadra, D., Chegrouche, S. and Lounici, H.: Investigation of aerosol trace element concentrations nearby Algiers for environmental monitoring using instrumental neutron activation analysis, Atmospheric Research, 166, 49–59, doi: 10.1016/j.atmosres.2015.06.013, 2015.

Cachier, H., Brémond, M.-P. and Buat-Ménard, P.: Carbonaceous aerosols from different tropical biomass burning sources, Nature, 340(6232), 371–373, doi:10.1038/340371a0, 1989.

Cachon, B. F., Firmin, S., Verdin, A., Ayi-Fanou, L., Billet, S., Cazier, F., Martin, P. J., Aissi, F., Courcot, D., Sanni, A. and Shirali, P.: Proinflammatory effects and oxidative stress within human bronchial epithelial cells exposed to atmospheric particulate matter (PM2.5 and PM>2.5) collected from Cotonou, Benin, Environmental Pollution, 185, 340–351, doi: 10.1016/j.envpol.2013.10.026, 2014.

Cao, J.J., Lee, S.C., Zhang, X.Y., Chow, J.C., An, Z.S., Ho, K.F., Watson, J.G., Fung, K., Wang, Y.Q. and Shen, Z.X.: Characterization of airborne carbonate over a site near Asian dust source regions during spring 2002 and its climatic and environmental significance, J. Geophys. Res., 110(D3), D03203, doi: 10.1029/2004JD005244, 2005.

Cassee, F. R., Héroux, M.-E., Gerlofs-Nijland, M. E. and Kelly, F. J.: Particulate matter beyond mass: recent health evidence on the role of fractions, chemical constituents and sources of emission, Inhalation Toxicology, 25(14), 802–812, doi:10.3109/08958378.2013.850127, 2013.

Celo, V., Dabek-Zlotorzynska, E., Mathieu, D., Okonskaia, I.: Validation of simple microwave-assisted acid digestion method using microvessels for analysis of trace elements in atmospheric PM 2.5 in monitoring and fingerprinting studies, The Open Chemical & Biomedical Methods Journal 3., 141–150, 2010.

Cesari, D., Donateo, A., Conte, M., Merico, E., Giangreco, A., Giangreco, F. and Contini, D.: An inter-comparison of PM2.5 at urban and urban background sites: Chemical characterization and source apportionment, Atmospheric Research, 174–175, 106–119, doi: 10.1016/j.atmosres.2016.02.004, 2016.

Cheng, Z., Jiang, J., Chen, C., Gao, J., Wang, S., Watson, J. G., Wang, H., Deng, J., Wang, B., Zhou, M., Chow, J. C., Pitchford, M. L. and Hao, J.: Estimation of Aerosol Mass Scattering Efficiencies under High Mass Loading: Case Study for the Megacity of Shanghai, China, Environ. Sci. Technol., 49(2), 831–838, doi: 10.1021/es504567q, 2015.

Chiang, H.-L., Lai, Y.-M. and Chang, S.-Y.: Pollutant constituents of exhaust emitted from light-duty diesel vehicles, Atmospheric Environment, 47, 399–406, doi: 10.1016/j.atmosenv.2011.10.045, 2012.

Chiapello, I., Bergametti, G., Chatenet, B., Bousquet, P., Dulac, F. and Soares, E. S.: Origins of African dust transported over the northeastern tropical Atlantic, J. Geophys. Res., 102(D12), 13701–13709, doi: 10.1029/97JD00259, 1997.

Chow, J. C., Watson, J. G., Lu, Z., Lowenthal, D. H., Frazier, C. A., Solomon, P. A., Thuillier, R. H. and Magliano, K.: Descriptive analysis of PM2.5 and PM10 at regionally representative locations during SJVAQS/AUSPEX, Atmospheric Environment, 30(12), 2079–2112, doi:10.1016/1352-2310(95)00402-5, 1996.

Colbeck, I., Nasir, Z. A., Ahmad, S. and Ali, Z.: Exposure to PM10, PM2.5, PM1 and Carbon Monoxide on Roads in Lahore, Pakistan, Aerosol Air Qual. Res., 11(6), 689–695, doi:10.4209/aaqr.2010.10.0087, 2011.

Colette, A., Menut, L., Haeffelin, M. and Morille, Y.: Impact of the transport of aerosols from the free troposphere towards the boundary layer on the air quality in the Paris area, Atmospheric Environment, 42(2), 390–402, doi: 10.1016/j.atmosenv.2007.09.044, 2007.

De Oliveira Alves, N., Brito, J., Caumo, S., Arana, A., de Souza Hacon, S., Artaxo, P., Hillamo, R., Teinilä, K., Batistuzzo de Medeiros, S. R. and de Castro Vasconcellos, P.: Biomass burning in the Amazon region: Aerosol source apportionment and associated health risk assessment, Atmospheric Environment, 120, 277–285, doi:10.1016/j.atmosenv.2015.08.059, 2015.

Dieme, D., Cabral-Ndior, M., Garçon, G., Verdin, A., Billet, S., Cazier, F., Courcot, D., Diouf, A. and Shirali, P.: Relationship between physicochemical characterization and toxicity of fine particulate matter (PM2.5) collected in Dakar city (Senegal), Environmental Research, 113, 1–13, doi:10.1016/j.envres.2011.11.009, 2012.

Ding, A., Huang, X. and Fu, C.: Air Pollution and Weather Interaction in East Asia, Oxford Research Encyclopedias-Environmental Sience, doi: 10.1093/acrefore/9780199389414.013. 536, 2017.

Djossou, J., Léon, J.-F., Akpo, A. B., Liousse, C., Yoboué, V., Bedou, M., Bodjrenou, M., Chiron, C., Galy-Lacaux, C., Gardrat, E., Abbey, M., Keita, S., Bahino, J., Touré N'Datchoh, E., Ossohou, M. and Awanou, C. N.: Mass concentration, optical depth and carbon composition of particulate matter in the major southern West African cities of Cotonou (Benin) and Abidjan (Côte d'Ivoire), Atmos. Chem. Phys., 18(9), 6275–6291, doi:10.5194/acp-18-6275-2018, 2018.

Draxler, R. R. and Rolph, G. D.: Evaluation of the Transfer Coefficient Matrix (TCM) approach to model the atmospheric radionuclide air concentrations from Fukushima: MODELING RADIONUCLIDES FROM FUKUSHIMA, J. Geophys. Res., 117(D5), n/a-n/a, doi: 10.1029/2011JD017205, 2012.

Du, Z., He, K., Cheng, Y., Duan, F., Ma, Y., Liu, J., Zhang, X., Zheng, M. and Weber, R.: A yearlong study of water-soluble organic carbon in Beijing I: Sources and its primary vs. secondary nature, Atmospheric Environment, 92, 514–521, doi:10.1016/j.atmosenv.2014.04. 060, 2014.

Favez, O. : Caractérisation physico-chimique de la pollution particulaire dans des mégapoles contrastées, Thèse de l'Université PARIS.DIDEROT (Paris 7), France, 2008.

Favez, O., Sciare, J., Cachier, H., Alfaro, S. C. and Abdelwahab, M. M.: Significant formation of water-insoluble secondary organic aerosols in semi-arid urban environment, Geophys. Res. Lett., 35(15), L15801, doi:10.1029/2008GL034446, 2008.

Feng, J., Guo, Z., Chan, C. K. and Fang, M.: Properties of organic matter in PM2.5 at Changdao Island, China—A rural site in the transport path of the Asian continental outflow, Atmospheric Environment, 41(9), 1924–1935, doi: 10.1016/j.atmosenv.2006.10.064, 2007.

Feng, J., Hu, M., Chan, C. K., Lau, P. S., Fang, M., He, L. and Tang, X.: A comparative study of the organic matter in PM2.5 from three Chinese megacities in three different climatic zones, Atmospheric Environment, 40(21), 3983–3994, doi: 10.1016/j.atmosenv.2006.02.017, 2006.

Foltescu, V. L., Selin Lindgren, E., Isakson, J., Öblad, M., Tiede, R., Sommar, J., Pacyna, J. M. and Toerseth, K.: Airborne concentrations and deposition fluxes of major and trace species at marine stations in Southern Scandinavia, Atmospheric Environment, 30(22), 3857–3872, doi:10.1016/1352-2310(96)00064-7, 1996.

Foner, H. A. and Ganor, E.: The chemical and mineralogical composition of some urban atmospheric aerosols in Israel, Atmospheric Environment. Part B. Urban Atmosphere, 26(1), 125–133, doi:10.1016/0957-1272(92)90045-T, 1992.

Freitas, M.C., Pacheco, A.M.G., Baptista, M.S., Dionísio, I., Vasconcelos, M.T.S.D. and Cabral, J.P.: Response of exposed detached lichens to atmospheric elemental deposition, Proc. ECOpole., 1(1/2), 15-21, 2007.

Gaga, E. O., Arı, A., Akyol, N., Üzmez, Ö. Ö., Kara, M., Chow, J. C., Watson, J. G., Özel, E., Döğeroğlu, T. and Odabasi, M.: Determination of real-world emission factors of trace metals, EC, OC, BTEX, and semivolatile organic compounds (PAHs, PCBs and PCNs) in a rural tunnel in Bilecik, Turkey, Science of The Total Environment, 643, 1285–1296, doi: 10.1016/j.scitotenv.2018.06.227, 2018.

Gao, Y., Nelson, E. D., Field, M. P., Ding, Q., Li, H., Sherrell, R. M., Gigliotti, C. L., Van Ry, D. A., Glenn, T. R. and Eisenreich, S. J.: Characterization of atmospheric trace elements on PM2.5 particulate matter over the New York–New Jersey harbor estuary, Atmospheric Environment, 36(6), 1077–1086, doi:10.1016/S1352-2310(01)00381-8, 2002.

Genga, A., Ielpo, P., Siciliano, T. and Siciliano, M.: Carbonaceous particles and aerosol mass closure in PM2.5 collected in a port city, Atmospheric Research, 183, 245–254, doi: 10.1016/j.atmosres.2016.08.022, 2017.

Gounougbe, F. : Pollution atmosphérique par les gaz d'échappement et état de santé des conducteurs de taxi-moto (Zemidjan) de Cotonou (Bénin), These de doctorat en Medecine(832), 1999.

1191 Guieu, C.: Chemical characterization of the Saharan dust end-member: Some biogeochemical
1192   implications for the western Mediterranean Sea, J. Geophys. Res., 107(D15), 4258, doi:
1193   10.1029/2001JD000582, 2002.

1194 Guinot, B., Cachier, H. and Oikonomou, K.: Geochemical perspectives from a new aerosol
1195   chemical mass closure, Atmos. Chem. Phys., 7(6), 1657–1670, doi: 10.5194/acp-7-1657-
1196   2007, 2007.

1197 Guttikunda, S. K. and Calori, G.: A GIS based emissions inventory at 1 km × 1 km spatial
1198   resolution for air pollution analysis in Delhi, India, Atmospheric Environment, 67, 101–
1199   111, doi:10.1016/j.atmosenv.2012.10.040, 2013.

1200 Hara, K., Osada, K., Kido, M., Hayashi, M., Matsunaga, K., Iwasaka, Y., Yamanouchi, T.,
1201   Hashida, G. and Fukatsu, T.: Chemistry of sea-salt particles and inorganic halogen species
1202   in Antarctic regions: Compositional differences between coastal and inland stations, J.
1203   Geophys. Res., 109, D20208, doi:10.1029/2004JD004713, 2004.

1204 He, K., Yang, F., Ma, Y., Zhang, Q., Yao, X., Chan, C. K., Cadle, S., Chan, T. and Mulawa, P.:
1205   The characteristics of PM2.5 in Beijing, China, Atmospheric Environment, 35(29), 4959–
1206   4970, doi: 10.1016/S1352-2310(01)00301-6, 2001.

1207 Herut, B., Nimmo, M., Medway, A., Chester, R. and Krom, M. D.: Dry atmospheric inputs of
1208   trace metals at the Mediterranean coast of Israel (SE Mediterranean): sources and fluxes,
1209   Atmospheric Environment, 35(4), 803–813, doi: 10.1016/S1352-2310(00)00216-8, 2001.

1210 Hildemann, L. M., Markowski, G. R. and Cass, G. R.: Chemical composition of emissions from
1211   urban sources of fine organic aerosol, Environ. Sci. Technol., 25(4), 744–759, doi:
1212   10.1021/es00016a021, 1991.

1213 Huang, H., Ho, K. F., Lee, S. C., Tsang, P. K., Ho, S. S. H., Zou, C. W., Zou, S. C., Cao, J. J.
1214   and Xu, H. M.: Characteristics of carbonaceous aerosol in PM2.5: Pearl Delta River
1215   Region, China, Atmospheric Research, 104–105, 227–236, doi:
1216   10.1016/j.atmosres.2011.10.016, 2012.

1217 Jaffrezo, J.-L., Aymoz, G., Delaval, C., and Cozic, J.: Seasonal variations of the Water Soluble
1218   Organic Carbon mass fraction of aerosol in two valleys of the French Alps, Atmos. Chem.
1219   Phys., 5, 2809–2821, 2005a.

1220 Keita, S., Liousse, C., Yoboué, V., Dominutti, P., Guinot, B., Assamoi, E.-M., Borbon, A.,
1221   Haslett, S. L., Bouvier, L., Colomb, A., Coe, H., Akpo, A., Adon, J., Bahino, J., Doumbia,
1222   M., Djossou, J., Galy-Lacaux, C., Gardrat, E., Gnamien, S., Léon, J. F., Ossohou, M.,
1223   N'Datchoh, E. T. and Roblou, L.: Particle and VOC emission factor
1224   measurements for anthropogenic sources in West Africa, Atmos. Chem. Phys., 18(10),
1225   7691–7708, doi:10.5194/acp-18-7691-2018, 2018.

1226 Khan, Md. F., Shirasuna, Y., Hirano, K. and Masunaga, S.: Characterization of PM2.5, PM2.5–
1227   10 and PM>10 in ambient air, Yokohama, Japan, Atmospheric Research, 96(1), 159–172,
1228   doi:10.1016/j.atmosres.2009.12.009, 2010.

10.5194/acp-2019-406
2019-06-11

Kim, H., Liu, X., Kobayashi, T., Kohyama, T., Wen, F.-Q., Romberger, D. J., Conner, H., Gilmour, P. S., Donaldson, K., MacNee, W. and Rennard, S. I.: Ultrafine Carbon Black Particles Inhibit Human Lung Fibroblast-Mediated Collagen Gel Contraction, Am J Respir Cell Mol Biol, 28(1), 111–121, doi:10.1165/rcmb.4796, 2003.

Knippertz, P., Tesche, M., Heinold, B., Kandler, K., Toledano, C. and Esselborn, M.: Dust mobilization and aerosol transport from West Africa to Cape Verde—a meteorological overview of SAMUM–2, Tellus B: Chemical and Physical Meteorology, 63(4), 430–447, doi:10.1111/j.1600-0889.2011. 00544.x, 2011.

Kouassi, K. S., Billet, S., Garçon, G., Verdin, A., Diouf, A., Cazier, F., Djaman, J., Courcot, D. and Shirali, P.: Oxidative damage induced in A549 cells by physically and chemically characterized air particulate matter (PM 2.5) collected in Abidjan, Côte d'Ivoire, J. Appl. Toxicol., n/a-n/a, doi:10.1002/jat.1496, 2009.

Laden, F., Neas, L. M., Dockery, D. W. and Schwartz, J.: Association of fine particulate matter from different sources with daily mortality in six U.S. cities. Environmental Health Perspectives, 108(10), 941–947, doi:10.1289/ehp.00108941, 2000.

Lamaison, L. : Caractérisation des particules atmosphériques et identification de leurs sources dans une atmosphère urbaine sous influence industrielle, Thèse Doctorat, Univ des Sciences et Technologies, Lille, 2006.

Laurent, B. : Simulation des émissions d'aérosols désertiques à l'échelle continentale : Analyse climatologique des émissions du nord-est de l'Asie et du nord de l'Afrique, Thèse de Doctorat, Université Paris 12, 2005.

Lee, S. W., Pomalis, R. and Kan, B.: A new methodology for source characterization of oil combustion particulate matter, Fuel Processing Technology, 65–66, 189–202, doi:10.1016/S0378-3820(99)00086-7, 2000.

Léon, J.F., Akpo, A., Bedou, M., Djossou, J., Bodjrenou, M., Yoboué, V., et Liousse, C. : Profondeur optique des aérosols sur le sud de l'Afrique de l'Ouest, soumis à ACPD, 2019.

Li, T.-C., Yuan, C.-S., Hung, C.-H., Lin, H.-Y., Huang, H.-C. and Lee, C.-L.: Chemical Characteristics of Marine Fine Aerosols over Sea and at Offshore Islands during Three Cruise Sampling Campaigns in the Taiwan Strait & amp;ndash; Sea Salts and Anthropogenic Particles, Atmos. Chem. Phys. Discuss., 1–27, doi:10.5194/acp-2016-384, 2016.

Li, Y., Schwandner, F. M., Sewell, H. J., Zivkovich, A., Tigges, M., Raja, S., Holcomb, S., Molenar, J. V., Sherman, L., Archuleta, C., Lee, T. and Collett, J. L.: Observations of ammonia, nitric acid, and fine particles in a rural gas production region, Atmospheric Environment, 83, 80–89, doi:10.1016/j.atmosenv.2013.10.007, 2014.

Liang, L., Engling, G., Du, Z., Cheng, Y., Duan, F., Liu, X. and He, K.: Seasonal variations and source estimation of saccharides in atmospheric particulate matter in Beijing, China, Chemosphere, 150, 365–377, 2016.

Liousse, C., Assamoi, E., Criqui, P., Granier, C., Rosset, R.: Explosive growth in African combustion emissions from 2005 to 2030, Environ. Res. Lett., 9, 035003, 2014.

Lonati, G., Ozgen, S. and Giugliano, M.: Primary and secondary carbonaceous species in PM2.5 samples in Milan (Italy), Atmospheric Environment, 41(22), 4599–4610, doi:10.1016/j.atmosenv.2007.03.046, 2007.

Lowenthal, D., Zielinska, B., Samburova, V., Collins, D., Taylor, N. and Kumar, N.: Evaluation of assumptions for estimating chemical light extinction at U.S. national parks, Journal of the Air & Waste Management Association, 65(3), 249–260, doi:10.1080/10962247.2014.986307, 2015.

Marinoni, A., Laj, P., Deveaux, P., Marino, F., Ghermandi, G., Aulagnier, F., and Cachier, H.: Physicochemical properties of fine aerosols at Pland'Aups during ESCOMPTE, Atmos.Res., 74, 565–580, 2005.

Mason, B., Moore, B.C.: Principles of Geochemistry, fourth ed. John Wiley and Sons, New York, pp. 46–47, 1982

Middleton, N. J., Betzer, P. R. and Bull, P. A.: Long-range transport of 'giant' aeolian quartz grains: linkage with discrete sedimentary sources and implications for protective particle transfer, Marine Geology, 177(3–4), 411–417, doi: 10.1016/S0025-3227(01)00171-2, 2001.

Minguillón, M. C., Cirach, M., Hoek, G., Brunekreef, B., Tsai, M., de Hoogh, K., Jedynska, A., Kooter, I. M., Nieuwenhuijsen, M. and Querol, X.: Spatial variability of trace elements and sources for improved exposure assessment in Barcelona, Atmospheric Environment, 89, 268–281, doi: 10.1016/j.atmosenv.2014.02.047, 2014.

Mkoma, S. L.: Physico-Chemical characterisation of atmospheric aerosols in Tanzania, with emphasis on the carbonaceous aerosol components and on chemical mass closure, PhD, Ghent University, Ghent, Belguim, 2008.

Mmari, A. G., Potgieter-Vermaak, S. S., Bencs, L., McCrindle, R. I. and Van Grieken, R.: Elemental and ionic components of atmospheric aerosols and associated gaseous pollutants in and near Dar es Salaam, Tanzania, Atmospheric Environment, 77, 51–61, doi: 10.1016/j.atmosenv.2013.04.061, 2013.

MMEH (Ministère des Mines de l'Energie et d'Hydraulique). : Tableau de bord de l'Energie 2002 au Bénin, Direction Générale de l'Energie, 2002.

Ngo, N. S., Asseko, S. V. J., Ebanega, M. O., Allo'o Allo'o, S. M. and Hystad, P.: The relationship among PM2.5, traffic emissions, and socioeconomic status: Evidence from Gabon using low-cost, portable air quality monitors, Transportation Research Part D: Transport and Environment, 68, 2–9, doi: 10.1016/j.trd.2018.01.029, 2019.

Ozer, P. : Estimation de la pollution particulaire naturelle de l'air en 2003 à Niamey (Niger) à partir de données de visibilité horizontale., 2005.

Pachauri, T., Singla, V., Satsangi, A., Lakhani, A. and Kumari, K. M.: Characterization of carbonaceous aerosols with special reference to episodic events at Agra, India, Atmospheric Research, 128, 98–110, doi: 10.1016/j.atmosres.2013.03.010, 2013.

Park, J. H., Mudunkotuwa, I. A., Mines, L. W. D., Anthony, T. R., Grassian, V. H. and Peters, T. M.: A Granular Bed for Use in a Nanoparticle Respiratory Deposition Sampler, Aerosol Science and Technology, 49(3), 179–187, doi:10.1080/02786826.2015.1013521, 2015.

Person, A & Tymen, G. : Mesurage des particules en suspension dans l'air en relation avec la santé. Pollution atmosphérique, 271-285, 2005.

Pettijohn, F.J.: Sedimentary Rocks. 2nd Edition, Harper and Row Publishers, New York, 628 p., 1975.

Pipal, A. S., Jan, R., Satsangi, P. G., Tiwari, S. and Taneja, A.: Study of Surface Morphology, Elemental Composition and Origin of Atmospheric Aerosols (PM2.5 and PM10) over Agra, India, Aerosol Air Qual. Res., 14(6), 1685–1700, doi:10.4209/aaqr.2014.01.0017, 2014.

Pipal, A. S., Singh, S. and Satsangi, G. P.: Study on bulk to single particle analysis of atmospheric aerosols at urban region, Urban Climate, 27, 243–258, doi: 10.1016/j.uclim.2018.12.008, 2019.

Prospero, J.M., Ginoux, P., Torres, O., Nicholson, S.E., Gill, T.E.: Environmental characterization of global sources of atmospheric soil dust identified with the NIMBUS 7 Total Ozone Mapping Spectrometer (TOMS) absorbing aerosol product, Rev Geophys, 40, 2-1-31, 2002.

Pulles, T., Denier van der Gon, H., Appelman, W. and Verheul, M.: Emission factors for heavy metals from diesel and petrol used in European vehicles, Atmospheric Environment, 61, 641–651, doi: 10.1016/j.atmosenv.2012.07.022, 2012.

Qin, Y., Chan, C. K. and Chan, L. Y.: Characteristics of chemical compositions of atmospheric aerosols in Hong Kong: spatial and seasonal distributions, Science of The Total Environment, 206(1), 25–37, doi: 10.1016/S0048-9697(97)00214-3, 1997.

Rengarajan, R., Sudheer, A. K. and Sarin, M. M.: Aerosol acidity and secondary organic aerosol formation during wintertime over urban environment in western India, Atmospheric Environment, 45(11), 1940–1945, doi: 10.1016/j.atmosenv.2011.01.026, 2011.

Renjian, Z., Jun, T., Ho, K.F., Zhenxing, S., Gehui, W., Junji, C., Suixin, L., Leiming, Z., Lee, S.C.: Characterization of atmospheric organic and elemental carbon of PM25 in a typical semi-arid area of Northeastern China, Aerosol Air Qual Res., 12, 792–802, 2012.

Sakata, M., Kurata, M. and Tanaka, N.: Estimating contribution from municipal solid waste incineration to trace metal concentrations in Japanese urban atmosphere using lead as a marker element. Geochem. J., 34(1), 23–32, doi:10.2343/geochemj.34.23, 2000.

Samara, C., Kouimtzis, T., Tsitouridou, R., Kanias, G. and Simeonov, V.: Chemical mass balance source apportionment of PM10 in an industrialized urban area of Northern Greece, Atmospheric Environment, 37(1), 41–54, doi:10.1016/S1352-2310(02)00772-0, 2003.

Satsangi, A., Pachauri, T., Singla, V., Lakhani, A. and Kumari, K. M.: Organic and elemental carbon aerosols at a suburban site, Atmospheric Research, 113, 13–21, doi: 10.1016/j.atmosres.2012.04.012, 2012.

Saxena, P., and Hildemann, L.M.: Water-soluble organics in atmospheric particles: a critical review of the literature and application of thermodynamics to identify candidate compounds, J. Atmos. Chem., 24(1), 57–109, 1996.

Schütz, L. and Rahn, K. A.: Trace-element concentrations in erodible soils, Atmospheric Environment (1967), 16(1), 171–176, doi: 10.1016/0004-6981(82)90324-9, 1982.

Sciare, J., Oikonomou, K., Cachier, H., Mihalopoulos, N., Andreae, M. O., Maenhaut, W. and Sarda-Estève, R.: Aerosol mass closure and reconstruction of the light scattering coefficient over the Eastern Mediterranean Sea during the MINOS campaign, Atmos. Chem. Phys., 5(8), 2253–2265, doi:10.5194/acp-5-2253-2005, 2005.

Seinfeld, J. H. et Pandis, S. N.: Atmospheric Chemistry and Physics: from Air Pollution to Climate Change, John Wiley and Sons, Inc. New York, 1998.

Sempére, R. and Kawamura, K.: Comparative distributions of dicarboxylic acids and related polar compounds in snow, rain and aerosols from urban atmosphere, Atmospheric Environment, 28(3), 449–459, doi:10.1016/1352-2310(94)90123-6, 1994.

Shahsavani, A., Naddafi, K., Jaafarzadeh Haghighifard, N., Mesdaghinia, A., Yunesian, M., Nabizadeh, R., Arhami, M., Yarahmadi, M., Sowlat, M. H., Ghani, M., Jonidi Jafari, A., Alimohamadi, M., Motevalian, S. A. and Soleimani, Z.: Characterization of ionic composition of TSP and PM10 during the Middle Eastern Dust (MED) storms in Ahvaz, Iran, Environ Monit Assess, 184(11), 6683–6692, doi:10.1007/s10661-011-2451-6, 2012.

Shen, Z., Cao, J., Zhang, L., Zhang, Q., Huang, R.-J., Liu, S., Zhao, Z., Zhu, C., Lei, Y., Xu, H. and Zheng, C.: Retrieving historical ambient PM2.5 concentrations using existing visibility measurements in Xi'an, Northwest China, Atmospheric Environment, 126, 15–20, doi: 10.1016/j.atmosenv.2015.11.040, 2016.

Sternbeck, J., Sjödin, Å. and Andréasson, K.: Metal emissions from road traffic and the influence of resuspension—results from two tunnel studies, Atmospheric Environment, 36(30), 4735–4744, doi: 10.1016/S1352-2310(02)00561-7, 2002.

Stone, R. S., Herber, A., Vitale, V., Mazzola, M., Lupi, A., Schnell, R. C., Dutton, E. G., Liu, P. S. K., Li, S.-M., Dethloff, K., Lampert, A., Ritter, C., Stock, M., Neuber, R. and Maturilli, M.: A three-dimensional characterization of Arctic aerosols from airborne Sun photometer observations: PAM-ARCMIP, April 2009, J. Geophys. Res., 115(D13), D13203, doi: 10.1029/2009JD013605, 2010.

Sullivan, A. P., Weber, R. J., Clements, A. L., Turner, J. R., Bae, M. S. and Schauer, J. J.: A method for on-line measurement of water-soluble organic carbon in ambient aerosol particles: Results from an urban site: ON-LINE MEASUREMENT OF WSOC IN AEROSOLS, Geophys. Res. Lett., 31(13), n/a-n/a, doi: 10.1029/2004GL019681, 2004.

Sun, Y., Zhuang, G., Wang, Y., Han, L., Guo, J., Dan, M., Zhang, W., Wang, Z. and Hao, Z.: The air-borne particulate pollution in Beijing—concentration, composition, distribution and sources, Atmospheric Environment, 38(35), 5991–6004, doi: 10.1016/j.atmosenv.2004.07.009, 2004.

Tang, X., Zhang, X., Ci, Z., Guo, J. and Wang, J.: Speciation of the major inorganic salts in atmospheric aerosols of Beijing, China: Measurements and comparison with model, Atmospheric Environment, 133, 123–134, doi: 10.1016/j.atmosenv.2016.03.013, 2016.

Tapsoba, D. : Caractérisation événementielle des régimes pluviométriques ouestafricains et de leur récent changement, Thèse de Doctorat, Univ.Paris-XI (Orsay). 100p, 1997.

Taylor, S. R.: Abundance of chemical elements in the continental crust: a new table, Geochimica et Cosmochimica Acta, 28(8), 1273–1285, doi: 10.1016/0016-7037(64)90129-2, 1964.

Terzi, E., Argyropoulos, G., Bougatioti, A., Mihalopoulos, N., Nikolaou, K. and Samara, C.: Chemical composition and mass closure of ambient PM10 at urban sites, Atmospheric Environment, 44(18), 2231–2239, doi: 10.1016/j.atmosenv.2010.02.019, 2010.

Tunno, B., Longley, I., Somervell, E., Edwards, S., Olivares, G., Gray, S., Cambal, L., Chubb, L., Roper, C., Coulson, G. and Clougherty, J. E.: Separating spatial patterns in pollution attributable to woodsmoke and other sources, during daytime and nighttime hours, in Christchurch, New Zealand, Environmental Research, 171, 228–238, doi: 10.1016/j.envres.2019.01.033, 2019.

Turpin, B. J., Cary, R. A. and Huntzicker, J. J.: An In Situ, Time-Resolved Analyzer for Aerosol Organic and Elemental Carbon, Aerosol Science and Technology, 12(1), 161–171, doi:10.1080/02786829008959336, 1990.

Union des villes et communes de Côte d'Ivoire (UVICOCI). : Revue de presse, Available at : http://uvicoci.ci/accueil/infopresse/1 (last access: 20 April 2019), 2018.

Val, S., Liousse, C., Doumbia, E. H. T., Galy-Lacaux, C., Cachier, H., Marchand, N., Badel, A., Gardrat, E., Sylvestre, A. and Baeza-Squiban, A.: Physico-chemical characterization of African urban aerosols (Bamako in Mali and Dakar in Senegal) and their toxic effects in human bronchial epithelial cells: description of a worrying situation, Part Fibre Toxicol, 10(1), 10, doi:10.1186/1743-8977-10-10, 2013.

Viana, M., López, J. M., Querol, X., Alastuey, A., García-Gacio, D., Blanco-Heras, G., López-Mahía, P., Piñeiro-Iglesias, M., Sanz, M. J., Sanz, F., Chi, X. and Maenhaut, W.: Tracers and impact of open burning of rice straw residues on PM in Eastern Spain, Atmospheric Environment, 42(8), 1941–1957, doi: 10.1016/j.atmosenv.2007.11.012, 2008.

Viana, M., Maenhaut, W., ten Brink, H. M., Chi, X., Weijers, E., Querol, X., Alastuey, A., Mikuška, P. and Večeřa, Z.: Comparative analysis of organic and elemental carbon concentrations in carbonaceous aerosols in three European cities, Atmospheric Environment, 41(28), 5972–5983, doi: 10.1016/j.atmosenv.2007.03.035, 2007.

Viidanoja, J., Sillanpää, M., Laakia, J., Kerminen, V.-M., Hillamo, R., Aarnio, P. and Koskentalo, T.: Organic and black carbon in PM2.5 and PM10: 1 year of data from an urban site in Helsinki, Finland, Atmospheric Environment, 36(19), 3183–3193, doi: 10.1016/S1352-2310(02)00205-4, 2002.

Voutsa, D., Samara, C., Kouimtzis, T. and Ochsenkühn, K.: Elemental composition of airborne particulate matter in the multi-impacted urban area of Thessaloniki, Greece, Atmospheric Environment, 36(28), 4453–4462, doi: 10.1016/S1352-2310(02)00411-9, 2002.

Wang, X., Bi, X., Sheng, G. and Fu, J.: Chemical Composition and Sources of PM10 and PM2.5 Aerosols in Guangzhou, China, Environ Monit Assess, 119(1–3), 425–439, doi: 10.1007/s10661-005-9034-3, 2006.

Washington, R., Todd, M., Middleton, N. J. and Goudie, A. S.: Dust-Storm Source Areas Determined by the Total Ozone Monitoring Spectrometer and Surface Observations, Annals of the Association of American Geographers, 93(2), 297–313, doi:10.1111/1467-8306.9302003, 2003.

Watson, J. G. and Chow, J. C.: Estimating middle-, neighborhood-, and urban-scale contributions to elemental carbon in Mexico City with a rapid response aethalometer, J Air Waste Manag Assoc, 51(11), 1522–1528, 2001.

Watson, J. G., Chow, J. C. and Houck, J. E.: PM2.5 chemical source profiles for vehicle exhaust, vegetative burning, geological material, and coal burning in Northwestern Colorado during 1995, Chemosphere, 43(8), 1141–1151, doi:10.1016/S0045-6535(00)00171-5, 2001.

Weckwerth, G.: Verification of traffic emitted aerosol components in the ambient air of Cologne (Germany), Atmospheric Environment, 35(32), 5525–5536, doi: 10.1016/S1352-2310(01)00234-5, 2001.

WHO (World Health Organization), 7 million premature deaths annually linked to air pollution. Media Centre news release. Geneva: World Health Organization. (http: //www.who.int/ mediacentre/news/releases/2014/airpollution/en/ (accessed 30 October 2014, accessed 2 April 2015), 2014.

Wilson, M. R., Lightbody, J. H., Donaldson, K., Sales, J. and Stone, V.: Interactions between ultrafine particles and transition metals in vivo and in vitro, Toxicol. Appl. Pharmacol., 184(3), 172–179, 2002.

Xiang, P., Zhou, X., Duan, J., Tan, J., He, K., Yuan, C., Ma, Y. and Zhang, Y.: Chemical characteristics of water-soluble organic compounds (WSOC) in PM2.5 in Beijing, China: 2011–2012, Atmospheric Research, 183, 104–112, doi: 10.1016/j.atmosres.2016.08.020, 2017.

Xiao, H.-Y., Shen, C.-Y., Zhang, Z.-Y. and Long, A.-M.: Chemical Composition and Sources of Marine Aerosol over the Western North Pacific Ocean in Winter, Atmosphere, 9(8), 298, doi:10.3390/atmos9080298, 2018.

Xie, Y., Wang, Y., Bilal, M. and Dong, W.: Mapping daily PM2.5 at 500 m resolution over Beijing with improved hazy day performance, Science of The Total Environment, 659, 410–418, doi: 10.1016/j.scitotenv.2018.12.365, 2019.

Xiu, G., Wu, X., Wang, L., Chen, Y., Yu, Y., Xu, F. and Wu, L.: Characterization of Particulate Matter, Ions and OC/EC in a Museum in Shanghai, China, Aerosol Air Qual. Res., 15(4), 1240–1250, doi:10.4209/aaqr.2014.07.0147, 2015.

Xu, H., Léon, J.-F., Liousse, C., Guinot, B., Yoboué, V., Akpo, A. B., Adon, J., Ho, K. F., Ho, S. S. H., Li, L., Gardrat, E., Shen, Z. and Cao, J.: Personal exposure to PM_{2.5} emitted from typical anthropogenic sources in Southern West Africa (SWA): Chemical characteristics and associated health risks, Atmos. Chem. Phys. Discuss., 1–68, doi:10.5194/acp-2018-1060, 2019.

Xu, J., Zhang, Y., Zheng, S. and He, Y.: Aerosol effects on ozone concentrations in Beijing: a model sensitivity study, J Environ Sci (China), 24(4), 645–656, 2012.

Yu, P., Froyd, K. D., Portmann, R. W., Toon, O. B., Freitas, S. R., Bardeen, C. G., Katich, J. M., Schwarz, J. P., Williamson, C., Kupc, A., Brock, C., Liu, S., Gao, R.-S., Schill, G., Fan, T., Rosenlof, K. H., and Murphy, D. M.: An improved treatment of aerosol convective transport and removal in a chemistry-climate model, Geophys. Res. Lett., submitted, 2018.

Zghaid, M., Noack, Y., Bounakla, M., and Benyaich, F.: Pollution atmosphérique particulaire dans la ville de Kenitra (Maroc), available at: http://lodel.irevues.inist.fr/ pollution-atmospherique/index.php?id=1184&format=print (last access: 24 May 2017), 2009.

Zhang, X. Y., Gong, S. L., Shen, Z. X., Mei, F. M., Xi, X. X., Liu, L.C., Zhou, Z. J., Wang, D., Wang, Y. Q., and Cheng, Y.: Characterization of soil dust aerosol in China and its transport and distribution during 2001 ACE-Asia: 1. Network observations, J. Geophys. Res.-Atmos., 108(D9), 4261, doi:10.1029/2002JD002632, 2003.

Zhang, X.-X., Sharratt, B., Liu, L.-Y., Wang, Z.-F., Pan, X.-L., Lei, J.-Q., Wu, S.-X., Huang, S.-Y., Guo, Y.-H., Li, J., Tang, X., Yang, T., Tian, Y., Chen, X.-S., Hao, J.-Q., Zheng, H.-T., Yang, Y.-Y. and Lyu, Y.-L.: East Asian dust storm in May 2017: observations, modelling, and its influence on the Asia-Pacific region, Atmos. Chem. Phys., 18(11), 8353–8371, doi:10.5194/acp-18-8353-2018, 2018.

1491

1492

1493

1494

Figure caption

Figure 1: Map of the city of Abidjan reporting the geographical location of DACCIWA urban sampling sites.

Figure 2: Map of the city of Cotonou reporting the geographical location of DACCIWA urban sampling site.

Figure 3: Pictures of the different sampling sites : (a) Traffic in Cotonou (Benin, CT station), (b) Waste burning in Abidjan (Côte d'Ivoire, AWB station), (c), Domestic fire, showing smoking activity in Yopougon, Abidjan (Côte d'Ivoire, ADF station), (d) " woro-woro and Gbaka " traffic in Abidjan (Côte d'Ivoire, AT station).

Figure 4: Wind, pressure and temperature diagram at Abidjan and Cotonou during the different campaigns.

Figure 5: Back trajectories arriving at Abidjan (a) and Cotonou (b) for each season (WS2015, WS2016, DS2016 and DS2017).

Figure 6: Aerosol Mass concentrations at the different study sites for each campaign and for the different sizes (C in black, Fine in light Grey, Ultra-fine in grey). aerosol mass is indicated in boxes.

Figure 7: Comparison of PM 2.5 mass concentrations in µg/m3 at the four sites with those obtained by Djossou et al. (2018) and Xu et al. (2019) for the same site and period.

Figure 8: EC relative concentrations in each size classes (C in black, Fine in light grey, Ultra-fine in grey) at the different study sites for each campaign. Bulk EC concentration for each site is indicated in boxes.

Figure 9: OC relative concentrations in each size classes (C in black, Fine in light grey, Ultra-fine in grey) at the different study sites for each campaign. Bulk OC concentration for each site is indicated in boxes.

1519   Figure 10: OC/ EC ratio for the different campaigns and sites for each aerosol size (C in black,
1520   Fine in light grey, Ultra-fine in grey). Each box shows the median and the first and the
1521   third quartiles.

1522   Figure 11: Water-soluble ionic species speciation for each site, each campaign and each aerosol
1523   size.

1524   Figure 12: Dust concentrations at the different study sites for each campaign and for the
1525   different sizes (C in black, Fine in light grey, Ultra-fine in grey).

1526   Figure 13: MODIS Aerosol optical depth regional distribution over West Africa. Data are for
1527   2017, focusing on our campaign date at Abidjan (a-c 01/11-12-left part) and Cotonou
1528   (b-d 01/6-7, right part).

1529   Figure 14: Size-speciated aerosol chemical composition for each site, for each campaign and
1530   each aerosol size.

1531

1532

1533

1534

1535

1536

1537

1538

1539

1540

1541

1542
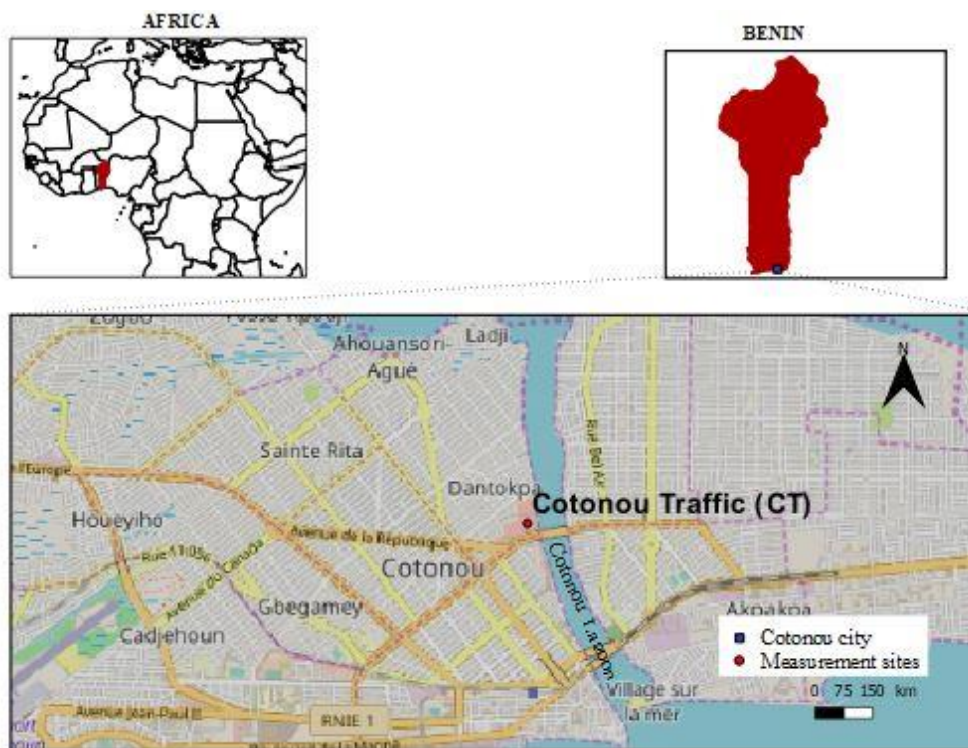
1543

1544

1545 Figure1
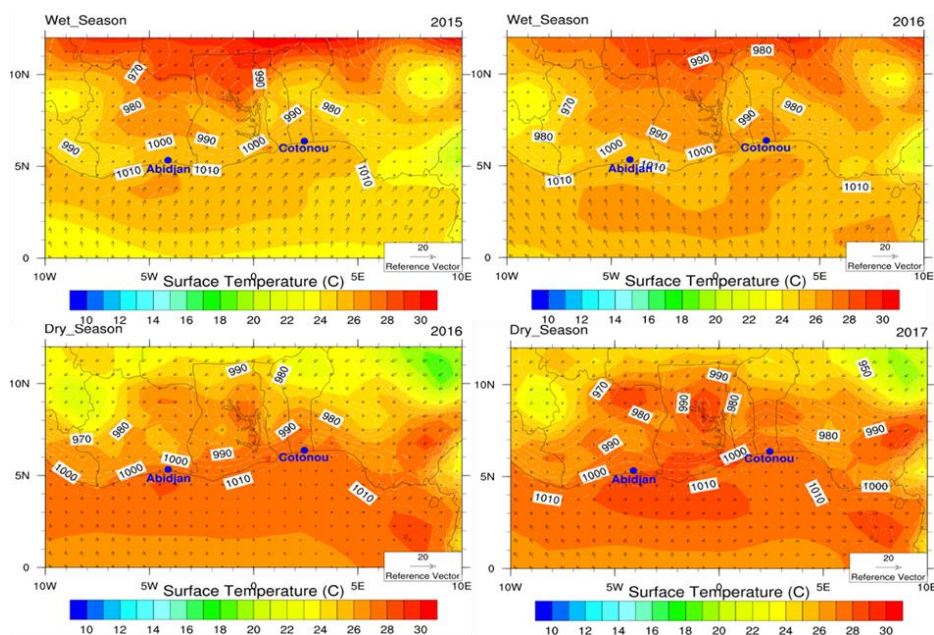
Figure 2

Figure 3

1570

1571

1572   **Figure 4**

1573

1574

1575

1576

1577

1578

1579

1580

1581

1582

1583

1584

1585

1586

1587

1588
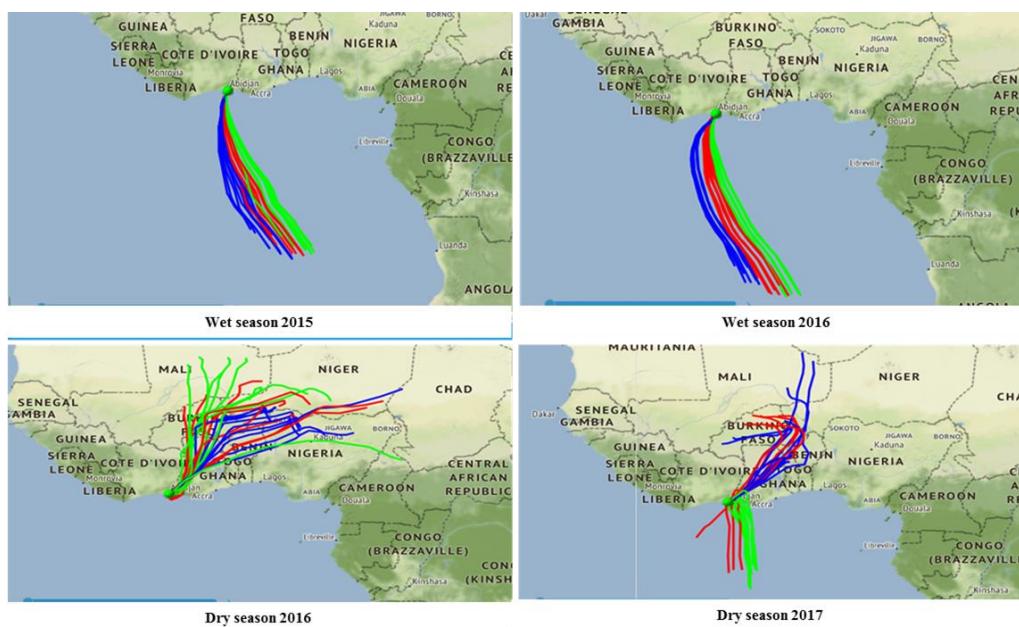
1589
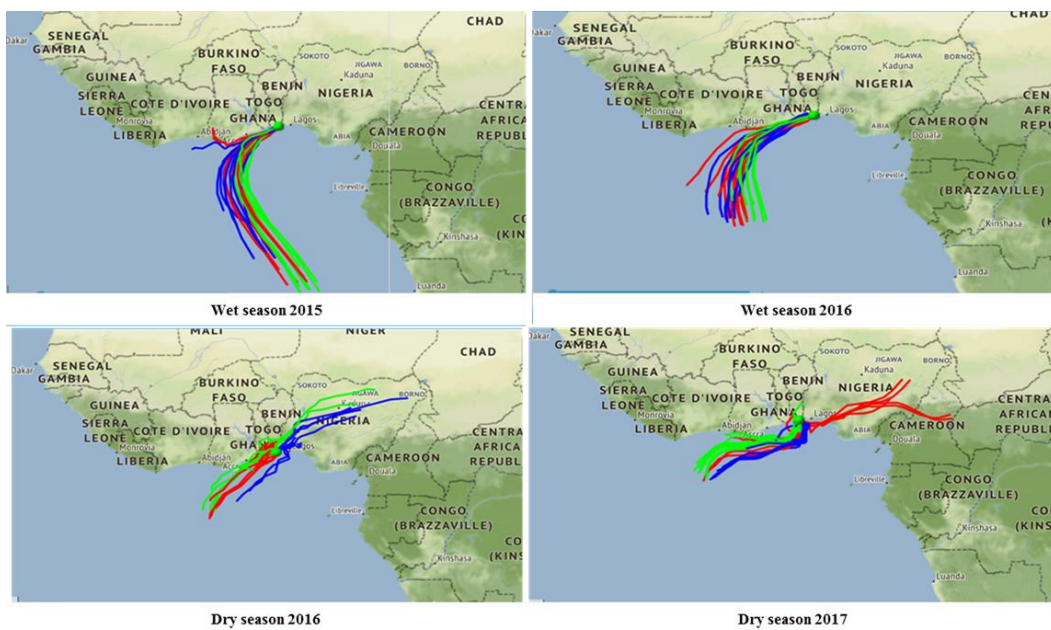
Figure 5-a

1591

Figure 5-b

1593

1594

1595

1596
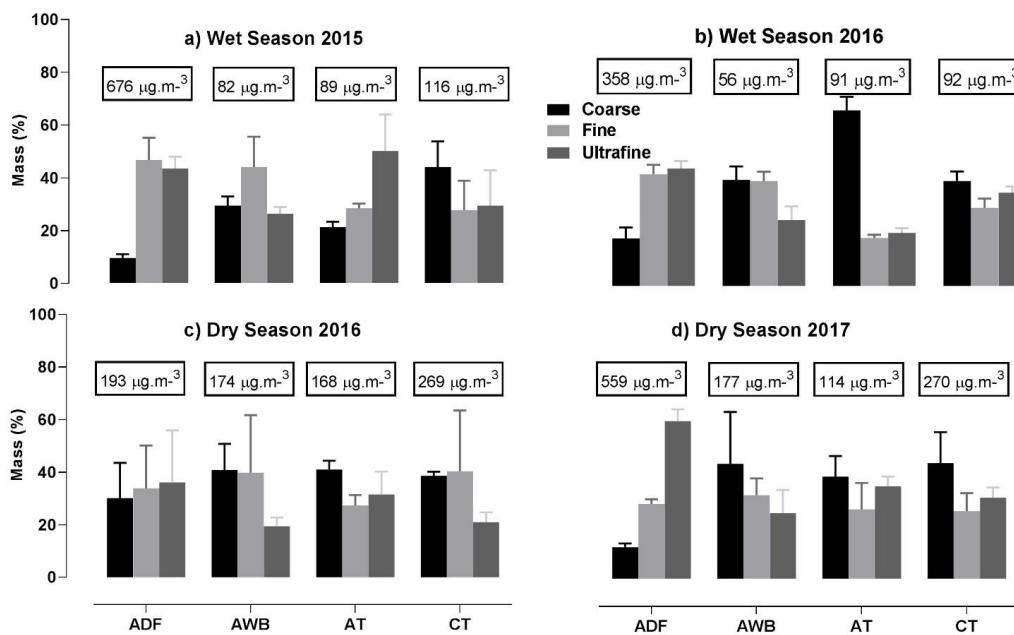
1597

1598   **Figure 6**

1599

1600
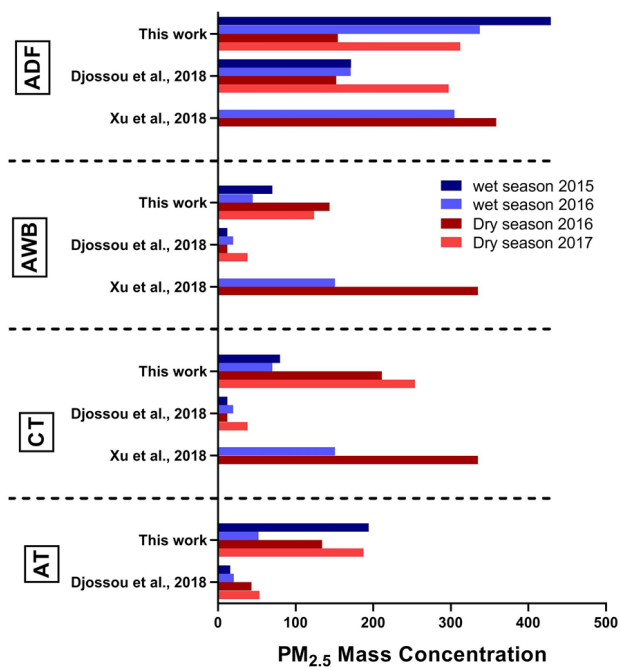
1601

1602   **Figure 7**

1603

1604

1605

1606
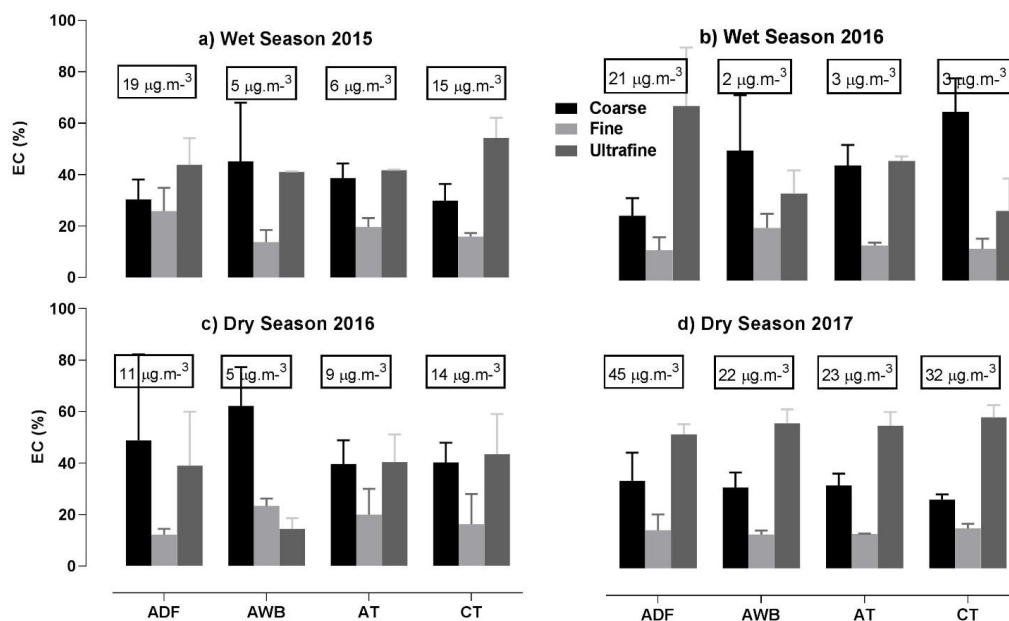
1607

1608 **Figure 8**

1609

1610

1611

1612

1613
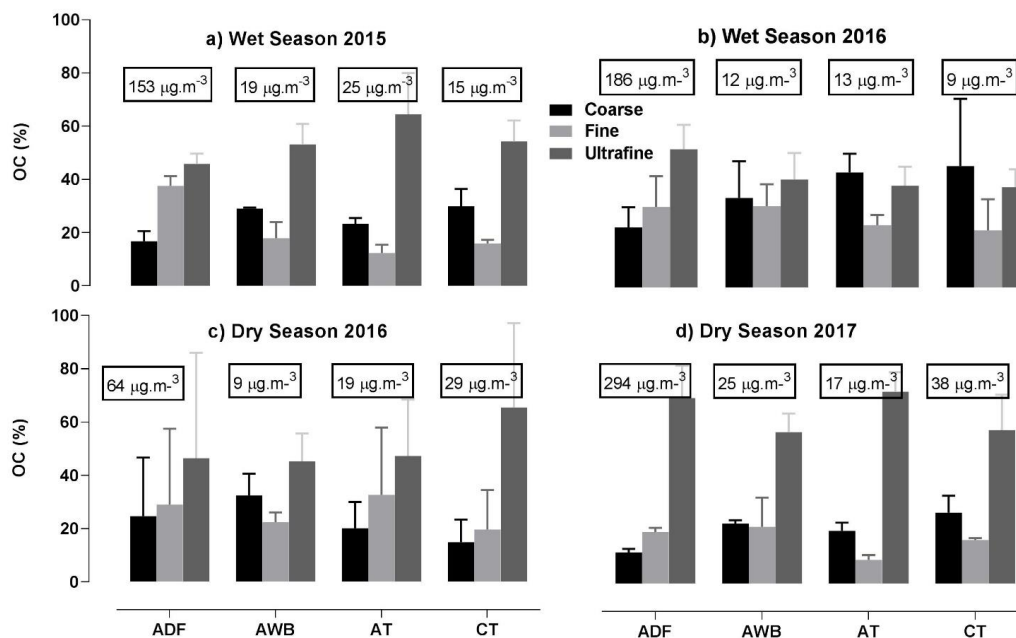
1614

Figure 9

1616

1617

1618

1619

1620
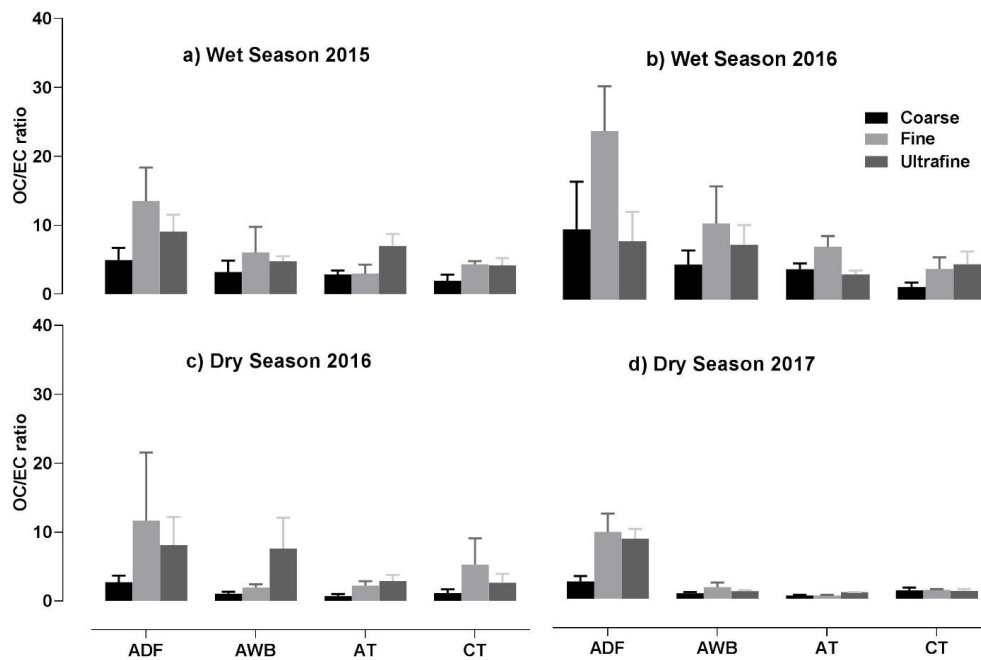
1621

1622   **Figure 10**

1623

1624
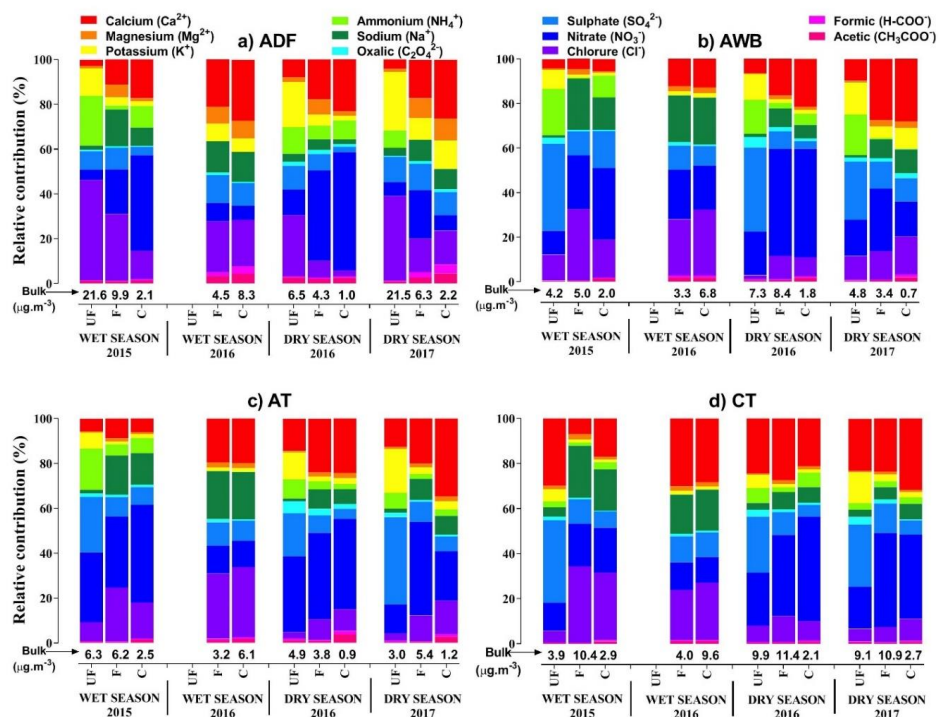
1625

1626   **Figure 11**
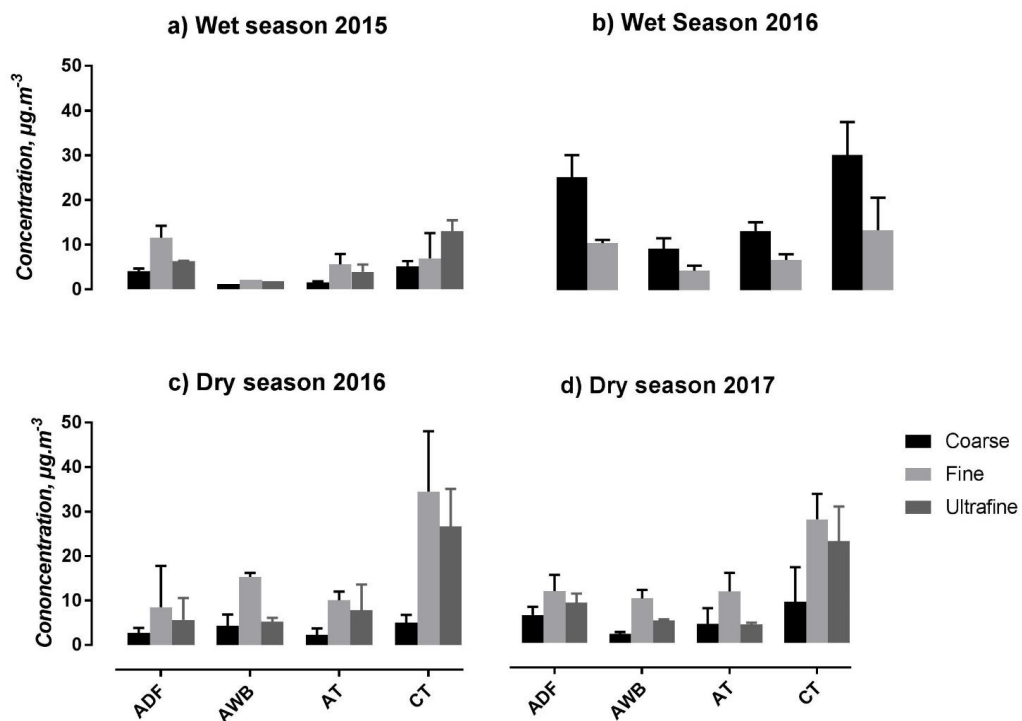
1627

1628   **Figure 12**

1629

1630
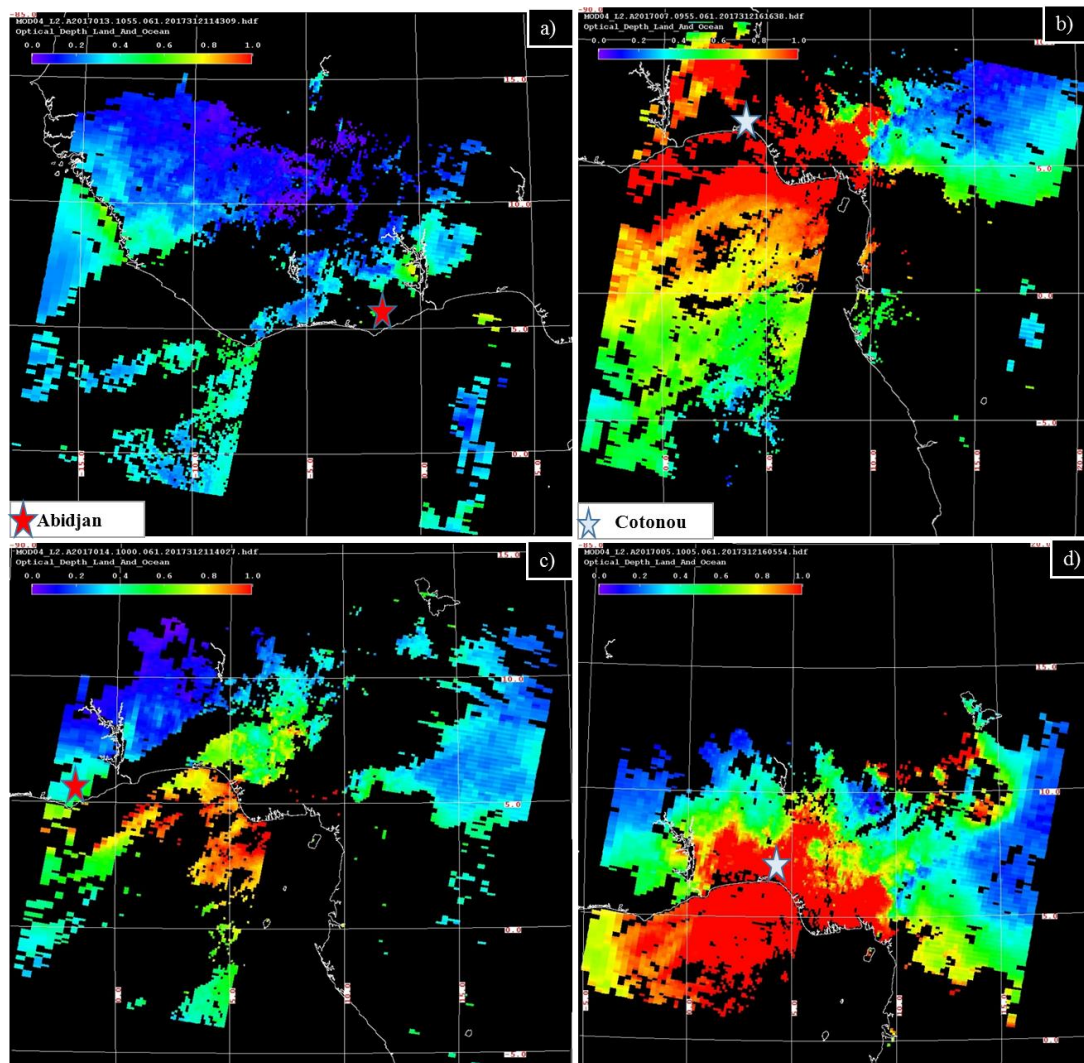
1631

1632   **Figure 13**
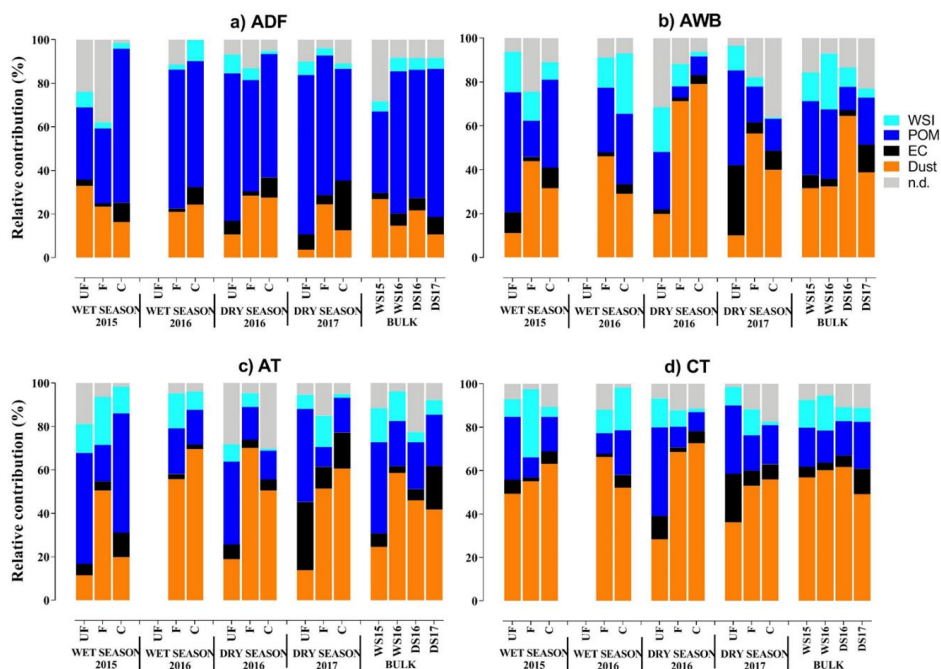
1633

1634   **Figure 14**

1635

1636

1637

1638

1639

1640

1641

1642

1643

1644

1645

1646

1647

1648

1649

1650

1651   Table 1: Comparison of dust concentrations obtained from different methodologies

Dry 2017		Pettijohn, 1975	Sciare et al. (2005)	Guinot et al. (2007)	Terzi et al. (2010)	Al	Fe
ADF	C	10.6	6.5	12.3	11.5	11.3	8.6
	F	81.5	12.0	38.6	75.4	110.3	27.6
	UF	15.8	9.3	8.4	22.2	20.2	6.5
	bulk	107.9	27.7	59.3	109.1	141.8	42.7
AWB	C	82.8	2.1	3.9	74.7	115.5	22.4
	F	57.6	10.2	32.8	51.7	75.8	51.1
	UF	118.4	5.2	31.9	106.4	164.0	21.7
	bulk	258.8	17.6	68.5	232.8	355.2	95.2
AT	C	55.6	4.5	5.5	50.3	76.6	9.0
	F	52.8	11.9	15.5	48.2	70.2	25.1
	UF	37.1	4.3	26.8	34.2	50.9	6.5
	bulk	145.5	20.7	47.8	132.7	197.7	40.7
CT	C	42.2	9.5	30.0	38.5	56.8	8.2
	F	65.1	28.4	-	59.9	84.2	43.1
	UF	58.6	23.4	66.0	55.8	77.3	33.8
	bulk	166.0	61.3	96.1	154.2	218.3	85.2

1652

Wet 2016		Pettijohn, 1975)	Sciare et al., 2005	Guinot et al., 2007	Terzi et al.(2010)	Al	Fe
ADF	C	13.1	25.0	14.2	15.4	10.6	16.0
	F	11.5	10.4	31.7	12.5	8.7	16.8
	UF	-	-	-	-	-	-
	Bulk	24.59	35.34	45.9	27.9	19.3	32.9
AWB	C	16.7	9.2	6.24	15.3	22.3	13.7
	F	6.0	4.3	9.82	5.7	5.8	4.0
	UF	-	-	-	-	-	-
	Bulk	22.65	13.46	16.1	21.1	28.1	17.7
AT	C	16.6	13.0	40.4	15.1	21.9	16.4
	F	6.9	6.7	8.87	6.3	9.0	8.3
	UF	-	-	-	-	-	-
	Bulk	23.45	19.65	49.22	21.4	30.9	24.7
CT	C	45.8	29.8	18.2	43.7	48.3	27.1
	F	8.7	13.2	17.2	8.8	8.3	11.6
	UF	-	-	-	-	-	-
	Bulk	54.51	42.98	35.4	52.5	56.6	38.7

1653 **Table 2**: Comparison of PM2.5 concentrations with literature data

Location	PM2.5 (µg/m³)	Reference
Abidjan, Côte d'Ivoire	142	This work
Cotonou, Benin	154	This work
Beijing, China	81.4	Xie et al., 2019
Christchurch, New Zealand	9.2	Tunno et al., 2019
Pune, India	98 ± 28	Pipal et al., 2019
Delhi, India	123	Guttikunda and Calori, 2013
Lahore, Pakistan	91	Colbeck et al., 2011
Ahvaz, Iran	69	Shahsavani et al., 2012
Hong Chong, Hong Kong	54.7 ± 25.6	Cheng et al., 2015
Lecce, Italia	16	Cesari et al., 2016
Libreville, Gabon	35.8	Ngo et al., 2019
Port Gentille, Gabon	60.9	Ngo et al., 2019
Kenitra, Morocco	51.3	Zghaid et al., 2009
Bilecik, Turkey	247	Gaga et al., 2018
Algiers, Algeria	34.8	Bouhila et al., 2015
Shobra, Egypt	216	Lowenthal et al.,2015

1654

1655

1656

1657   **Table 3**: PM2.5-EC and PM2.5-OC comparison with Djossou et al. (2018) and Xu et al. (2019)
1658   values. Units are µgC/m³.

Location	Period	PM2.5 OC	PM2.5 EC	References
Traffic Abidjan. Cote d'Ivoire	July 2015	22.6 ± 3.4	4.3 ± 0.2	This Work
	January 2016	15.2 ± 5.3	7.0 ± 2.6	
	July 2016	9.3 ± 1.3	2.2 ± 0.1	
	January 2017	16.1 ± 1.7	18.9 ± 1.4	
	July 2015	3.3 ± 0.2	2.3 ± 0.2	Djossou et al. 2018
	January 2016	7.7 ± 0.0	3.9 ± 0.0	
	July 2016	7.6 ± 0.2	4.9 ± 0.0	
	January 2017	19.1 ± 6.2	13.9 ± 5.5	
Traffic Cotonou. Benin	July 2015	13.1 ± 1.2	3.5 ± 0.7	This Work
	January 2016	27.8 ± 11.3	10.9 ± 2.6	
	July 2016	6.7 ± 1.9	2.0 ± 0.5	
	January 2017	33.1 ± 4.6	27.3 ± 0.9	
	July 2015	4.2 ± 0.7	1.5 ± 0.1	Djossou et al. 2018
	January 2016	3.0 ± 0.3	1.5 ± 0.2	
	July 2016	6.7 ± 0.2	1.6 ± 0.1	
	January 2017	14.5 ± 0.8	4.4 ± 0.7	
	January 2016	49.5 ± 12.5	13.6 ± 3.6	Xu et al. 2019
	July 2016	37.0 ± 3.5	9.3 ± 0.8	
Domestic fire Abidjan. Cote d'Ivoire	July 2015	147.2 ± 14.5	16.1 ± 1.6	This Work
	January 2016	56.5 ± 51.5	7.4 ± 3.1	
	July 2016	172.3 ± 39.0	17.9 ± 4.8	
	January 2017	283.9 ± 34.9	37.9 ± 4.3	
	July 2015	80.5 ± 1.1	32.2 ± 1.6	Djossou et al. 2018
	January 2016	76.3 ± 13.7	11.4 ± 0.2	
	July 2016	68.4 ± 16.5	17.4 ± 2.1	
	January 2017	66.4 ± 7.5	21.1 ± 6.6	
	January 2016	72.4 ± 24.6	19.5 ± 7.3	Xu et al. 2019
	July 2016	189.3 ± 197.8	11.5 ± 10.8	
Waste Burning Abidjan. Cote d'Ivoire	July 2015	14.8 ± 1.1	4.4 ± 0.1	This Work
	January 2016	7.7 ± 1.3	3.0 ± 0.3	
	July 2016	10.0 ± 2.4	1.5 ± 0.3	
	January 2017	21.9 ± 4.2	19.2 ± 2.4	
	July 2015	3.7 ± 2.2	4.3 ± 0.3	Djossou et al. 2018
	January 2016	13.9 ± 9.0	3.6 ± 1.8	
	July 2016	9.8 ± 4.4	2.8 ± 0.9	
	January 2017	22.4 ± 7.8	8.7 ± 3.0	
	January 2016	85 ± 57.4	15 ± 4.7	Xu et al. 2019
	July 2016	65.2± 65.2	12.3 ± 11.4	

1659

1660

1661

1662 **Table 4:** EC and OC comparison with literature values

Location	OC (µg/m³)	BC (µg/m³)	Reference
Abidjan (Côte d'Ivoire)	16	8.1	This study
Cotonou (Benin)	20.2	11	This study
Bilecik (Turkey)	49.6-62.8	38.8-58.1	Gaga et al., 2018
Pune (India)	30	5	Pipal et al., 2019
Shanghai (China)	4.9-13.1	1.9-5	Ding et al., 2017
Lahore (Pakistan)	85.7-152	13.8-21	Stone et al., 2010
Agra (India)	25.4-70	3.3-9.5	Satsangi et al., 2012, Pipal et al., 2014
Delhi (India)	34.1-50	5.3-10.6	Bisht et al., 2015a, Pipal et al., 2014
Ahmedabad (India)	18.3	3	Rengarajan et al., 2011
Yokohama (Japan)	4	2	Khan et al., 2010
Beijing (China)	2.9-28.2	1.2-16.3	Guinot et al., 2007

1663

1664

Table 5: WSOC concentrations and WSOC/OC ratios for each site, each campaign and each aerosol size

Site		Abidjan Waste Burning		Abidjan Domestic Fire	
Period	**Size**	**WSOC (µg/m³)**	**WSOC/OC (%)**	**WSOC (µg/m³)**	**WSOC/OC (%)**
Wet season 2015	Coarse	1.3	24,6	8.2	32.5
	Fine	0.7	19.9	12.8	22.7
	Ultra fine	4.1	43.6	51.3	72.5
	PM2.5	5.5	33.7	69.5	47.2
Dry season 2016	Coarse	0.4	12.3	4.4	18.8
	Fine	0.9	46.9	7.0	20.4
	Ultra fine	1.5	38.4	21.9	61.5
	PM2.5	2.7	32.7	31.0	32.0
Wet season 2016	Coarse	1.3	42.5	16.5	44.3
	Fine	0.8	26.3	17.1	33.0
	Ultra fine	2.0	41.2	79.7	84.5
	PM2.5	3.5	37.1	106.0	52.0
Dry season 2017	Coarse	1.9	32.9	12.1	36.0
	Fine	1.4	38.4	19.9	35.0
	Ultra fine	1.6	11.5	38.6	19.0
	PM2.5	4.0	30.0	65.8	29.0

Table 5 (suite): WSOC concentrations and WSOC/OC ratios for each site, each campaign and each aerosol size

Site		Abidjan Traffic		Cotonou Traffic	
Period	**Size**	**WSOC (µg/m³)**	**WSOC/OC (%)**	**WSOC (µg/m³)**	**WSOC/OC (%)**
Wet season 2015	Coarse	2.4	39.6	1.1	23.3
	Fine	1.3	46.7	0.5	22.1
	Ultra fine	4.7	29.0	0.4	12.7
	PM2.5	6.9	34.0	2.2	18.0
Dry season 2016	Coarse	1.4	43.0	2.3	64.1
	Fine	1.9	59.0	0.6	10.5
	Ultra fine	4.9	62.0	6.3	42.9
	PM2.5	7.5	49.4	8.0	29.0
Wet season 2016	Coarse	1.1	23.1	1.2	34.7
	Fine	0.5	16.8	0.5	32.2
	Ultra fine	1.4	34.8	0.9	23.0
	PM2.5	2.4	26.0	1.9	28.0
Dry season 2017	Coarse	0.9	24.0	3.5	37.8
	Fine	0.3	24.3	2.4	39.6
	Ultra fine	1.8	14.8	1.9	10.4
	PM2.5	2.6	16.0	6.0	18.2

1671

1672   **Table 6**: Comparison of WSOC concentrations with literature data

Location	WSOC (µg/m³)	Reference
Abidjan, Côte d'Ivoire	2-8	This work
Cotonou, Benin	2-8	This work
Beijing, China	9-27	Yu et al., 2018
Beijing, China	4-6	Xiang et al., 2017
Beijing, China	8-12	Tang et al., 2016
Beijing, China	7	Du et al., 2014
Beijing, China	6-8	Feng et al., 2006
Shanghai, China	2-7	Feng et al., 2006, Huang et al., 2012
Guangzhou, Hong Kong	2	Huang et al., 2012
Guangzhou, Hong Kong	5-10	Feng et al., 2006
Gwangju, Korea	2-3.5	Park et al., 2015
Tokyo, Japan	3-23	Sempere and Kawamura, 1994
Cairo, Egypt	3	Favez et al., 2008
Amsterdam, Netherland	1-2	Feng et al., 2007
Barcelone, Spain	1-2	Viana et al., 2007 and 2008
Brindisi, Italy	1.5	Genga et al., 2017
Saint Jean de Maurienne, France	1-5	Sullivan et al., 2004, Jaffrezo et al., 2005a

1673

1674

1675 **Table 7** : Trace element concentrations for bulk aerosol for each site and for DS2017 and WS2016

	Bulk ng/m³ (%)							
	DRY 2017				WET 2016			
	ADF	AWB	AT	CT	ADF	AWB	AT	CT
Al	10050.8 (1.8)	25186.1 (13.7)	14015.8 (12.26)	15480.4 (5.7)	1370.5 (0.4)	1990.1 (3.5)	2191.4 (2.4)	4010.5 (4.4)
K	8634.3 (1.5)	6093.7 (3.3)	3677.7 (3.22)	5068.9 (1.9)	1105.0 (0.3)	472.0 (0.8)	275.9 (0.3)	1076.0 (1.2)
Na	6847.8 (1.2)	23430.5 (12.8)	15372.1 (13.44)	11529.3 (4.3)	2070.6 (0.6)	3735.4 (6.6)	2861.5 (3.1)	5310.2 (5.8)
Ca	4321.2 (0.8)	2923.7 (1.6)	4117.6 (3.60)	6233.5 (2.3)	4124.7 (1.1)	447.5 (0.8)	374.7 (0.4)	4954.02 (5.4
Mg	1940.6 (0.3)	384.0 (0.2)	410.3 (0.36)	823.2 (0.3)	1524.7 (0.4)	294.9 (0.5)	283.5 (0.3)	619.2 (0.7)
Fe	1709.9 (0.3)	3807.9 (2.1)	1628.1 (1.42)	3406.8 (1.3)	1314.0 (0.4)	709.3 (1.3)	987.3 (1.1)	1549.4 (1.7)
P	1521.9 (0.3)	696.0 (0.4)	147.8 (0.13)	207.4 (0.1)	605.4 (0.2)	8.6	13.2	81.4 (0.1)
Ti	488.9 (0.1)	2270.3 (1.2)	282.8 (0.25)	457.9 (0.17)	170.8 (0.05)	75.7 (0.13)	96.8 (0.11)	154.7 (0.17)
Zn	189.7 (0.03)	80.9 (0.04)	57.9 (0.05)	149.4 (0.06)	60.3 (0.02)	1.9	41.1 (0.04)	36.2 (0.04)
Zr	172.1 (0.03)	390.3 (0.21)	217.9 (0.19)	145.3 (0.05)	-	22.4 (0.04)	36.7 (0.04)	31.2 (0.03)
Pb	87.1 (0.02)	11.0 (0.01)	4.8	11.5	8.3	2.1	2.3	9.3 (0.01)
Sn	79.7 (0.01)	38.4 (0.02)	21.6 (0.02)	37.4 (0.01)	0.77	0.09	0.0006	9.ç (0.01)
Mn	74.2 (0.01)	35.2 (0.02)	33.7 (0.03)	160.6 (0.06)	48.9 (0.01)	12.01 (0.02)	9.1 (0.01)	41.41 (0.05)
Rb	52.4 (0.01)	8.7	5.9 (0.01)	8.5	4.47	0.71	0.85	1.9
Sb	59.9 (0.01)	201.2 (0.11)	123.6 (0.11)	149.04 (0.06)	24.4 (0.01)	0	0.0006	2.9
Ba	37.3 (0.01)	53.3 (0.03)	47.4 (0.04)	65.8 (0.02)	18.5	8.02 (0.01)	9.9 (0.01)	32.0 (0.03)
Ni	36.5 (0.01)	34.5 (0.02)	27.9 (0.02)	50.2 (0.02)	18.00)	33.1 (0.06)	9.7 (0.01)	14.9 (0.02)
Cr	29.4 (0.01)	53.8 (0.03)	35.8 (0.03)	28.6 (0.01)	41.9 (0.01)	47.7 (0.08)	24.3 (0.03)	29.7 (0.03)
Sr	28.1 (0.01)	15.5 (0.01)	21.2 (0.02)	34.02 (0.01)	17.02	0	0.19	8.1 (0.01)
Cu	24.0	12.3 (0.01)	3.6	9.6	3.99	0.26	0.87	2.8)
Sr	12.6	-	-	-	17.1	-	0.22	8.9 (0.01)
Li	7.3	15.5 (0.01)	7.8 (0.01)	7.39	0.36	0.32	0.23	0.75
Cd	6.1	1.6	1.0	0.83	1.18	0.05	0.02	0.17
V	5.5	12.4 (0.01)	5.1	10.62	2.14	1.84	2.0	3.35
Mo	5.5	8.0	4.9	3.19	4.56	6.84 (0.01)	2.04	3.2
Cs	5.4	0.9	1.2	0.94	0.11	0.12	0.01	0.17
Hf	4.5	10.8 (0.01)	6.8 (0.01)	4.63	0	0.67	1.03	0.97
As	4.2	4.5	3.1	1.22	0	0 (0)	0.05	0.60
Li	4.0	9.8	5.9 (0.01)	5.82	0.27	0.37	0.16	0.93
Co	3.8	1.1	2.1	35.67 (0.01)	0.86	0.49	0.13	0.33
Ce	3.7	6.8	6.0 (0.01)	9.85	1.06	0.50	0.42	2.03
La	1.8	3.5	2.9	4.78	0.54	0.24	0.25	0.92
Nb	1.5	2.6)	1.4	2.48	0.98	0.46	0.5	0.63
Nd	1.5	2.5	2.4	4.15	0.05	0 (0)	-	0.40
Sc	0.69	1.4	1.1)	1.31		0,00		0.02
Be	0.13	0.19	0.2	0.28	0.003	-	-	0.03
Ga	0.61	1.15	0.8	0.98	0.2	0.11	0.12	0.37
Ge	0.42	1.02	0.8	0.68	0.01	0.07	0.02	0.11
Se	0.91	-	-	0.02	0.59	-	0.20	0.18
Rh	0.02	0.02	0.00002	0.002	-	0.002		0.0002
Te	0.06	0.08	0.08	0.05	0.02	0.02	0.02	0,00
Pr	0.40	0.74	0.7	1.13	0.06	0.01	0.004	0.15
Sm	0.27	0.46	0.45	0.76	0.01	0,00	-	0.07
Eu	0.05	0.08	0.08	0.15	0.01	0.003	--	0.0
Gd	0.31	0.57	0.54	0.86	0.05	0.02	0.001	0.15
Tb	0.04	0.07	0.07	0.10	0.005	-	-	0.02
Dy	0.24	0.42	0.40	0.57	0.001	-	-	0.05
Ho	0.05	0.09	0.09	0.12	0.01	0.008	0.01	0.03
Er	0.16	0.31	0.28	0.35	0.02	0.03	0.02	0.09

Tm	0.02	0.05	0.05	0.05	0.002	0.003	0.001	0.01
Yb	0.18	0.38	0.32	0.34	0.01	0.02	0.03	0.09
Lu	0.03	0.06	0.08	0.06	0.003	0.005	0.005	0.02
Ta	0.07	0.14	0.09	0.16	0.06	0.02	0.02	0.03
W	0.80	1.63	0.69	0.54	0.26	0.41	0.4	0.3
Tl	0.22	0.01	0.03	0.06		0.009		
Bi	0.32	0.26	0.02	0.08	0.06	-	-	0.08
Th	0.41	0.88	0.79	1.29	0.15	0.09	0.09	0.24
U	0.22	0.43	0.49	0.51	0.03	0.03	0.02	0.09
Total	36459.9	65817.6	40312.2	44159.2	12562.9	7874.7	7227.2	18001.1
Mass(μg/m^3)	558.8	183.6	114.4	270.0	374.7	56.3	91.6	91.9

1676

1677

1678

Table 8: Selected trace element ratios for bulk particles, for each site and for WS2016 and DS2017

	ADF		AWB		AT		CT	
	WET 2016	**DRY 2017**	**WET 2016**	**DRY 2017**	**WET 2016**	**DRY 2017**	**WET 2016**	**DRY 2017**
Cu/Sb	0.28 ± 0.21	0.56 ± 0.21	-	0.08 ± 0.08	1982.3 ± 1743.7	0.02 ± 0.01	0.57	0.19 ± 0.16
As/V	-	0.78 ± 0.17	-	0.41 ± 0.10	0.07	0.29 ± 0.01	0.15 ± 0.19	0.15 ± 0.06
V/Ni	0.13 ± 0.03	0.21 ± 0.16	0.04 ± 0.01	0.36 ± 0.16	0.28 ± 0.15	0.16 ± 0.02	0.46 ± 0.37	0.33 ± 0.17
Zn/Pb	7.1 ± 3.4	2.8 ± 1.3	2.30	13.2 ± 5.6	19.9 ± 14.7	14.8 ± 3.8	3.26 ± 2.31	18.5 ± 8.5
Zn/Cd	133.9 ± 109.4	29.1 ± 5.3	19.6 ± 25.9	55.9 ± 17.3	3932 ± 5061	51.7 ± 5.2	200±122	266.5±130.9